UNIVERSITY OF CALIFORNIA
RIVERSIDE

Ionothermal Synthesis of Lithium Iron Phosphate Composite Nanoparticles as a Cathode Material for Li-ion Batteries

A Thesis submitted in partial satisfaction
of the requirements for the degree of

Master of Science

in

Materials Science and Engineering

by

Ian Jacob Miller

March 2015

Thesis Committee:
Dr. Alfredo Martinez-Morales, Co-Chairperson
Dr. Cengiz Ozkan, Co-Chairperson
Dr. Mihri Ozkan
Dr. Juchen Guo

The Thesis of Ian Jacob Miller is approved:

Committee Co-Chairperson

Committee Co-Chairperson

University of California, Riverside

Acknowledgements

First and foremost, I would like to acknowledge my family for their support and assistance with my degrees and this Master's thesis. Without them, I could not have accomplished this phenomenal feat.

Next, I would like to thank Dr. Alfredo Martinez-Morales who has given me the chance to fulfill my dream of obtaining a Master's Degree in the field of materials. He has been extremely patient with me and has supported me through every peak and valley. Thank you for affecting my life so profoundly.

My thanks to Mr. Winston Chung who generously funded my particular project, and the projects of my colleagues, through the Winston Chung Global Energy Center. I also would like to thank my committee members, Dr. Cengiz Ozkan and Dr. Mihri Ozkan, and Dr. Juchen Guo who have agreed to be a part of my committee and helped me through this journey. I would also like to thank the department of Materials Science and Engineering, in particular Ms. Katie Dell and Dr. Ludwig Bartels for their insight and knowledge.

My special thanks to my lab mates Mr. Taehoon Lim and Mr. Darren Kwee who assisted me with SEM, EDS, XRD and the synthesis of my cathode material. Without these two great individuals, completing my thesis on time would have been impossible. A final thanks to CE-CERT faculty, staff, and students who have been extremely friendly and supportive. This facility truly is a family, who work well together and interact very well.

Table of Contents

List of Tables

List of Figures

1.0 Introduction

1.1 General Battery Background

The first modern battery was invented in 1800 by Alexander Volta, called the Voltaic pile. Around the same time the Leyden Jar was invented by Pieter van Musschenbroek [1]. The Leyden Jar was the first modern capacitor. A metal electrode was submerged in an electrolyte and connected to a foil lining in the jar to complete a circuit. Although this modern capacitor was invented in 1745, similar devices have been discovered dating back over 5,000 years. Clay pots found in what is modern day Iraq could have possibly been used as batteries but were probably used for electroplating to coat jewelry in gold and silver [2, 3]. Although these batteries had three main components of a modern battery, an electrolyte and two electrodes, modern energy storage devices have many more applications than early batteries. Today energy storage devices, especially batteries, are found in cell phones, computers, watches, medical equipment, airplanes, cars and even in space craft. Batteries are vital as portable energy storage apparatuses that can power very small or very large electronic devices.

Before one can talk about the different types of batteries that have been developed throughout the decades, one has to understand the battery operation mechanism. These energy storage devices convert chemical potential energy into electrical energy to perform useful work. There are three main components of a battery: a) a positive terminal called a cathode, b) a negative terminal called

an anode and c) a separator material (usually a liquid). The separator material helps facilitate the chemical reaction or acts as a medium for charge carriers to move from one terminal to another. A battery generates electricity through chemical reactions that occur between the electrode [4].

Daily use of batteries has become common place. They are used to charge and power electronic devices such as alarm clocks, remote controls, cell phones and radios. Various electronic devices have different voltage and energy requirements. This is evidenced by types of batteries carried in stores such as AA, AAA, C, and D batteries which are primary batteries designed for a one time use. These classifications refer to the potential and current of the packaged battery. Lead-acid, nickel metal oxide, and most lithium ion batteries are referred to as secondary batteries that are rechargeable [5, 6]. Each battery type, regardless of primary or secondary types, have different voltage and current specifications defined by the amount and type of electrode materials utilized.

1.2 Emphasis of Project

Battery research is crucial for the development of energy storage for use in devices on the small and large scales. Reserves of fossil fuels are quickly diminishing because of the ever growing demand for energy. Eventually our technologically driven society will have to wean itself off the use of fossil fuels and rely more heavily on renewable sources such as wind and solar energies. Although wind and solar energy solutions are sustainable, and will ensure a long lasting energy source, these technologies have their drawbacks. For one, solar

and wind energies are not always constant and they are intermittent in nature. During the night or on a cloudy day, photovoltaic cells will not produce energy and when there is no wind; energy cannot be drawn from wind turbines. The ability to store energy from these technologies is essential to ensure power is available at all times.

New powerful portable technologies are driving energy storage device research since energy storage devices are important on the small scale as well as the large scale. New devices such as computers and now smart phones, smart pads, and smart watches will become ever more important in our everyday lives. The ability to power these devices is also a challenge because the current trend of technologies seems to be getting smaller. The capability to manufacture and scale up or down a material that provides long cycle life, and more energy per unit weight, will ensure that energy storage devices can keep up with new technologies.

The specific emphasis of my project is on the novel synthesis, with an emphasis on industrial manufacturing, of $LiFePO_4$/C cathode materials with greater energy density while employing fewer or no toxic metals. Lithium-ion batteries have been a transformative technology for energy-intensive applications such as hybrid-electric and pure-electric automobiles. Their cost is a barrier to widespread adoption, and their use of toxic metals mitigates their environmental benefits. Common transition metals in lithium batteries today are cobalt [7], nickel

[8], and manganese [9], all of which are either toxic or rare. My research will use iron as the transition metal for the cathode, eliminating this health and environmental risk [10] and reducing the need for expensive materials.

$LiFePO_4$ is an excellent material for use as a cathode in a lithium ion battery due to its high specific capacity (170 mAh/g) [11] as well as its benign toxicity. Adding a carbon matrix to $LiFePO_4$ increases the electrical conductivity by 6 orders of magnitude which improves the performance during cycling and in overall charge capacity of the cathode [12-22]. The synthesis route, described in this dissertation, could enable an enhanced performing energy storage material to be created at a lower cost. Ionothermal synthesis allows for the liquid medium, an ionic liquid, to be recovered post synthesis using HPLC [23] which reduces the cost of manufacturing. The low temperatures and low synthesis time needed to create $LiFePO_4$ also reduces the cost leading to an ideal method for mass production of an energy storage material.

1.3 How Batteries Work

The general convention of powering a device using a battery, called discharging, occurs when current flows from the cathode to the device where the electrons perform electrical work to power the device. The anode then completes the circuit needed for the discharging process where the electrons flow in the opposite direction. The flow of total charge passing through a device per unit time, which by convention is opposite to electron flow, is called current which is

usually measured in milliamps. The total amount of charge that can be held in a device is measured in mA*h. Potential or voltage is the measurement of electric potential energy per unit charge. Voltage is the electric equivalent of force in classical mechanics. The difference in voltage between two points is equal to the work or energy required to move the charge divided by the magnitude of the charge.

It's not only useful to understand how a battery works chemically, it is also very important to understand how a battery can be applied to a system. A great practical example is that if you need to power a small motor with a battery that has a total charge of 1,000 mA*h and a potential of 3.5V volts, and your electric motor runs at 3 watts, how long would your battery operate the motor?

The general equation for power is: P = IV where P is power, I is current in amps and V is voltage. To power this motor with the given parameters, we can find out how long the battery will last.

$$3\ Watts = X\ amps \times 3.5\ Volts$$

The current required for one hour of operation is 850 mA so if we use the relationship,

$$\frac{850\ mA}{3600\ s} = \frac{1000\ mA}{y\ s} \qquad y = 4235.3\ s\ or\ 1\ hour\ and\ 10\ minutes$$

This means that the battery can power the motor for approximately 1 hour and 10 minutes. When looking at different batteries to be used in a process, one

must take into account how they will be used and whether or not they can power the intended device.

Batteries employ different mechanisms by which cells convert chemical energy to working electrical energy. Chemical reactions within the system, charging and discharging capabilities (also known as specific energy) and specific capacity (total energy that can be stored per unit of mass) all differ between various battery types. One must consider all of these factors when creating new battery materials or when using a battery within a particular system. A discussion of the genesis of batteries is very useful in order to understand the challenges that face current energy storage devices.

1.4 Lead Acid Batteries

One of the first commercially available batteries, which are still used in automobiles today, are lead acid batteries. Lead acid batteries have three different components: the anode which is a pure lead plate, the cathode which is a lead sulfate ($PbSO_4$) plate and the electrolyte which is sulfuric acid H_2SO_4 [24, 25]. Discharging a lead-acid battery begins when sulfuric acid chemically reacts with the pure lead plate, resulting in a lead sulfate plate and a very dilute solution of sulfuric acid. Charging the battery would have a reverse reaction resulting in a concentrated solution of sulfuric acid and a pure lead plate. The chemical reaction between the lead plate and the sulfuric acid generates electrons used in powering the desired device [24, 25].

There are many downsides to lead acid batteries. Lead acid batteries have a low power to weight ratio. This limitation means that they can't hold a lot of charge per unit mass. A typical car battery consists of 6 cells which add up to 9 lbs on average. Many cells must be used in series because the normal cell potential is 2.1 V per cell and at least 6 cells are required to obtain a 12V battery used in most automobiles today. Lead-acid batteries don't have great specific power or energy (180 W/Kg, 30–40 Wh/kg respectively) or the voltage per unit mass that is necessary for low-weight high-power applications. Additionally, lead is very toxic and is known to be a carcinogen making it very dangerous with which to work. The electrolyte used to facilitate the electrochemical reaction is an extremely caustic and strong acid: Sulfuric acid. A special liner has to be incorporated within the battery to contain these harmful materials while in use. Over time the degradation of the battery can contaminate the environment with toxic solvents and heavy metals. Due to the electrodes and electrolyte used in lead-acid batteries, combined with a low specific power and energy, a production of an energy storage device to power phones or computers is physically impossible [26].

1.5 Nickel Metal Oxide Batteries

The next development in the history of energy storage was the nickel cadmium and nickel metal oxide batteries. They were a great improvement over lead acid batteries because they have greater specific capacities, greater potential between electrodes and are less toxic than lead acid batteries. Nickel-

Cadmium batteries, named for the nickel hydroxide and pure cadmium electrodes, were an improvement over lead-acid batteries mainly because of its specific power and energy (150 W/kg, 40–60 W·h/kg respectively [27]). However lead, cadmium, and nickel are highly toxic elements to the environment and living organisms [27, 28] which eliminates these battery types as viable options for a sustainable future. The storage capacity of nickel cadmium and nickel metal oxide batteries is greater than lead acid but poor compared to the next development.

1.6 Lithium Ion Batteries

Lithium Ion batteries were first proposed by M.S Whittingham in the 1970's while working at Exxon [29]. It was discovered that lithium ion batteries don't react by creating covalent bonds in a reversible reaction that drives previous energy storage devices. Lithium ion batteries are named for the mechanism in which energy is stored and released; lithium ions are imbedded within a crystal structure and diffuse in/out of the material acting as a charge carrier. These lithium ions when charged will de-intercalate from an electrode, usually the cathode, allowing the electrode to hold a charge. After that there is a built up of charge on the electrode up to a certain potential, depending on the cathode material used, the devices can be discharged to release workable energy. Lithium ions diffuse between electrodes, usually from anode to cathode, which will intercalate into the crystal structure of the electrode releasing a single electron per lithium ion.

In the early 1990's, rechargeable lithium ion batteries were developed by John Goodenough and Koichi Mizushima [30] in which a lithium cobalt oxide cathode and a pure lithium anode were used. Currently lithium ion batteries use graphite in anode electrodes since using pure lithium at higher temperatures is a fire hazard. Lithium ion batteries offered huge advances in performance, more exactly their specific power and energy improvements (250-340 W/kg, 100–265 W·h/kg respectively [31]. This meant that batteries could perform more useful work without the restriction of being bulky or weighing too much, allowing hand held electronic devices such as lap tops and smart phones to be widely used.

Calculating specific power and energy is not as straight forward and easy as one might think. The density functional theory, or DFT, is used to calculate these parameters and usually differ between materials and their crystal structure. Many lithium ion batteries are therefore differentiated by their specific capacity, which is the measure of their total current capacity per unit mass (mA*h/g, see above for examples and explanation). There is also a difference between the theoretical and operating specific capacity of a particular material depending on how many lithium ions are extracted/intercalated before causing permanent deformation or irreversibly damaging of the cathode. For cathode materials such as Li_xCoO_2, the ability to exhibit comparable cycling exists when $1<x<0.5$ which limits the specific capacity of this material to 138-140 mA*h/g. In comparison, the theoretical specific capacity is 273 mA*h/g making this particular cathode material very limited [32].

Other proposed lithium-ion cathodes contain transition metals such as nickel, manganese, and a combination of metals such as $LiNi_{0.5}Mn_{1.5}O_2$. These transition metals, particularly cobalt and nickel, are toxic materials and are potentially hazardous to the environment and to living organisms. Heavy metals could easily contaminate the water table or leech into the soil, creating a health and environmental hazard. Using iron as the transition metal for our material eliminates this health and environmental risk due to toxic metal contamination. $LiFePO_4$ is also a naturally occurring non-toxic mineral called triphylite, making $LiFePO_4$ an efficient and environmentally friendly choice for a cathode material.

1.7 Benefits of $LiFePO_4$ as a Cathode Material

A lithium iron phosphate cathode material has many advantages to other proposed cathode materials that are currently being studied. Many new cathode materials contain elements such as cobalt, manganese, and nickel. Even though these materials can be used to make effective batteries they lack one key feature, sustainability. These metals contained in the battery are ultratrace elements, which are found in nature and are essential components in biological systems, but if consumed in large quantities can become toxic [33]. These metals are classified as ultratrace due to the fact that extremely small quantities can conceivably be dangerous to humans and animals if consumed. Iron found in our cathode material is also a trace element but it is not an ultratrace element. Ultratrace elements are much more dangerous than trace elements because smaller quantities of these materials can harm organisms.

Most lithium ion batteries have a relatively short lifetime, about one to three years depending on the charge and discharge rates [34]. As the demand for these batteries increases, larger numbers of spent batteries will enter our landfills as they are deployed [35]. Batteries can be recycled and this is definitely the most responsible thing to do. However, the government has classified lithium ion batteries as non-hazardous waste that can be disposed of in landfills and municipal waste streams [36]. After many years of these batteries being manufactured and discarded, the chance of these materials entering our water supply is greatly increased [37]. If batteries are made with these ultratrace materials, the risk for water contamination and for human and animal health issues increases. $LiFePO_4$ batteries are also known to have a longer life than traditional batteries because the life of the battery does not depend on the high state of charge [30].

1.8 Lithium Ion Mechanism

Lithium ion batteries differ from other types of batteries mainly due to the method in which useable electrons are generated. Where most other batteries use a chemical reaction between an electrode and an electrolyte to generate electrons, lithium ion batteries diffuse lithium ions into and out of the crystal structure of an electrode. Electrolyte solutions are merely separators and ion conductors between the two electrodes and are not meant to chemically react with either electrode. In $LiFePO_4$ batteries, lithium ions diffuse out of the base crystal structure creating a $FePO_4$ matrix and collect near the anode during

charging. Lithium ions diffuse back into the crystal structure, releasing a single electron per lithium atom which is used to perform work on the device being powered [38]. This mechanism is portrayed in Figure 1.

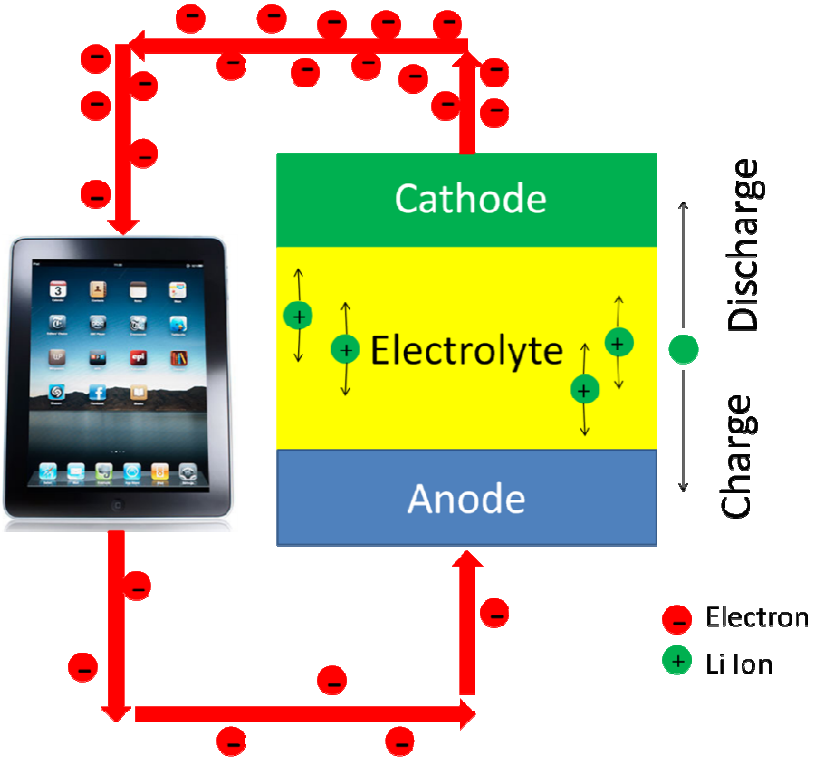

Figure 1: Mechanism of a Lithium Ion Battery

1.9 Improvements to $LiFePO_4$

To improve cycling and capacity performance, this research focused on the ionothermal synthesizes of carbon coated $LiFePO_4$ nanoparticles as a cathode material for lithium ion batteries. Lithium ion cathode materials operate when lithium ions diffuse into or out of the crystal structure, depending on charging or discharging, generating electrons used to perform work in a system (i.e. iPad or

computer). Increasing the surface area of the cathode material by synthesizing nanoparticles will allow for greater lithium ion diffusion into/out of the crystal structure, thus allowing greater performance per unit mass. Ionothermal synthesis of $LiFePO_4$ nanoparticles is a simple and cost effective method to create affordable and high performance energy storage devices. In addition, a carbon coating will improve the conductivity of $LiFePO_4$ which is an insulating olivine. A sol-gel component is added post precipitation of $LiFePO_4$, which adds a sp^2 hybridized carbon matrix, improving the electrical conductivity by many orders of magnitude. Carbon coating of nanoparticles also offers greater mechanical strength relaxing the strain on the particles during charging/discharging. This added mechanical strength will prevent the cathode material from deforming when cycling at higher rates.

1.10 Role of Ionic Liquid During Synthesis

Ionic liquids are organic solvents composed solely of ions which are liquids at room temperature. All ionic liquids share similar traits, such as high thermal stability, high salvation capacity, and high ionic conductivity [39-43] compared to aqueous solutions. Ionic liquids are also thought to facilitate growth of certain materials by oxidizing certain species within a mixture [44]. Though all ionic liquids share common traits, modifying the cations and anions that comprise these organic solvents can drastically change individual properties of the liquid [46-47]. The ability for a certain ionic liquid to be tailored designed for a particular process is one of the most attractive prospects in utilizing ionic liquids.

Some of the most critical traits desired in an ionic liquid to facilitate the growth of $LiFePO_4$ were temperature stability over 200°C, high ionic conductivity, and cost. Ionothermal and electrochemical synthesis of $LiFePO_4$ has been achieved with the ionic liquid 1-ethyl-3-methylimidazolium bis(trifluoromethylsulfonyl)imide by Yunhua Chen et al, but encountered some very practical problems. The cost of this particular ionic liquid is over $150/g (>97% through Sigma Aldrich) which limits the amount of $LiFePO_4$ that can be synthesize and eliminates the ability to use an ionothermal method for industrial applications. In addition to high cost, this particular ionic liquid starts to thermally decompose around 275°C. This particular trait is detrimental to synthesis conditions over 0.1M concentrations.

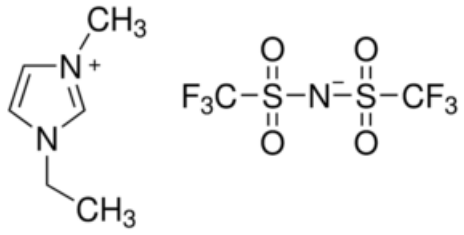

Figure 2: Chemical structure of 1-ethyl-3-methylimidazolium bis(trifluromethylsulfonlyl)imidie

To mimic the advantageous traits of 1-ethyl-3-methylimidazolium bis(trifluoromethylsulfonyl)imide, shown in Figure 2, while addressing cost and temperature constraints, an extensive study of ionic liquids was conducted. The most thermally stable ionic liquid found at an affordable price was 1-ethyl-3-methylimidazolium triflouromethanesulfonate, which is shown in Figure 3. This

particular ionic liquid works well in the synthesis of $LiFePO_4$ as the decomposition temperature is over 300°C while maintaining high ionic conductivity [42]. The price per gram is also significantly less than other comparable ionic liquids, $1.20/g (>98% through Sigma Aldrich). The novel ionothermal synthesis of $LiFePO_4$ will be investigated using 1-ethyl-3-methylimidazolium triflouromethanesulfonate due to the high thermal stability, high ionic conductivity, ability to oxidize iron species, and the price.

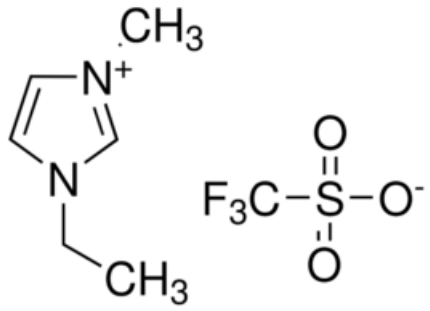

Figure 3: Chemical structure of 1-ethyl-3-methylimidazolium trifluoromethanesulfonate

2. Synthesis Plan & Experimentation

2.1 Background on Synthesis Methods

Many synthesis methods for $LiFePO_4$ have been previously explored, but a variety of methods have particular strengths and weaknesses. The most common and widely used method to obtain ceramics, such as phospho-olivines, is by solid state reaction. This method is easily scalable for mass production and is a very straight forward method involving heat treatment, grinding, and sintering at temperatures between 300-800°C [5, 48, 49]. However, long synthesis time and high temperature requirements make this an inefficient method for mass production of $LiFePO_4$ [54].

Sol-gel synthesis methods have also been achieved by mixing multiple precursors in a medium that is originally a liquid and through mixing, turns into a gel. The sol-gel is then heated between 500-700°C for up to 24 hours. This method allows for excellent mixing of precursors which produces uniform nanoparticle particles both in size and composition [50, 51]. However this method is rather complicated and does not easily scale to full production. Large energy and time requirements make this particular synthesis method unattractive to large scale manufacturing [54].

Hydrothermal and solvothermal methods involve synthesis with mediums such as water or organic solvents to dissolve precursors, increasing the surface

area during reaction. Precursors, along with the medium, are placed in an autoclave or bomb reaction vessel and heated to temperatures between 100-250°C under high pressure. Heating can be done either in a conventional oven or a microwave oven that can heat up specific molecules. Drawbacks for this method include long synthesis times, high pressure reaction vessels, and long post-synthesis processing [54, 52].

Solvothermal method comprises of one or multiple precursors as well as an ionic liquid medium not containing water (if an aqueous solution is used, the method is called hydrothermal) heated under atmospheric pressure to precipitate a material. The liquid allows the precursors to diffuse more easily which reduces the energy and time required to fully complete the reaction [54]. Completing synthesis through a solvothermal method has many advantages, including low temperature requirements, ease of handling, and a 99% yield of product [53]. Ionothermal synthesis is a subsection of solvothermal synthesis in which an ionic liquid is used to dissolve precursors instead of an aqueous solution. However previous ionothermal methods have required up to 24 hours reaction time and the use of extremely expensive ionic liquids such as 1-ethyl-3-methylimidazolium bis(trifluoromethylsulfonyl)imide [53, 54]. The ionothermal synthesis route we are proposing requires only a 1 hour reaction time and an affordable ionic liquid, 1-ethyl-3-methylimidazolium trifluoromethanesulfonate, which is attractive for large scale manufacturing due to the low cost of the synthesis.

Ionothermal synthesis is very similar to a solvothermal method but a molten salt, known as an ionic liquid, is used as the liquid medium. Ionic liquids are salts with anions and cations similar to NaCl, or table salt, that are liquids at room temperature. Relatively high temperatures can be achieved, at or above 300°C depending on the particular salt, which creates relatively high crystalline products compared to hydrothermal methods. The different cations and anions play specific roles in the morphology of the synthesized crystal as well, allowing for finely tuned products of purity and crystallinity.

As well as controlling the morphology of the $LiFePO_4$ nanoparticles, adding SP^2 hybridized carbon in the form of a matrix can greatly improve conductivity and cycling performance [56]. $LiFePO_4$ has an olivine crystal structure which belongs to a family of electrically insulating crystal structures. To assist electron conduction from the insulating $LiFePO_4$ crystal to the current collector, a very small amount of a carbon is added post synthesis of the nanoparticles. The beauty of adding a carbon matrix after synthesis is the simplicity and quickness of the process. Adding starch to $LiFePO_4$ material and heating it to 500°C for 2 hours, 90% of the theoretical maximum specific capacity can be achieved, which is around 160mAh/g. This inexpensive and quick method improves the performance of the nanoparticles greatly, cutting down on manufacturing costs and improving throughput. The expected total time from synthesis to the end of processing is a total of 6 hours. Some hydrothermal

methods take up to 24 hours to synthesize the material, let alone process the material.

Other possible carbonization methods include adding sugar [57], sucrose [58], or glucose [59, 60] before synthesis of $LiFePO_4$ which has been proven to enhance the overall performance of the material [60]. This performance increase is attributed to carbon matrices creating nucleation sites resulting in smaller crystallites of $LiFePO_4$ [65-97]. Electron motions in crystals follow grains, or rows of a set of molecules within a particular crystal. However when an amorphous material is produced, electron motion is random resulting in a longer time for an electron to perform useful work [98]. Having a crystalline material is very beneficial when charging or discharging at higher rates not only for quicker electron exchange, but also for material stability [60]. Although adding carbon pre-synthesis has many advantages, it has a few major drawbacks for our process.

When working with a carbon precursor for electrochemical improvement, one has to take into consideration carbonization. The process of heating a carbon source to form a carbon matrix is called carbonization. This carbon matrix is what provides extra stability as well as improving conductivity of the system. Both the sugar and sucrose method require carbonization at temperatures above 500°C, which is higher than the boiling point of our ionic liquid. Sugar, sucrose, and glucose is insoluable into the ionic liquid which eliminates a pre-synthesis

method to obtain growth of a $LiFePO_4$/C composite. A post-synthesis method could work in creating carbon coated nanoparticles however a solid state reaction would yield an uneven coverage of carbon [57 - 60].

2.2 Synthesis of $LiFePO_4$

The proposed method for synthesis in this work is focused on an ionothermal approach. Two precursors, iron chloride ($FeCl_3$) and lithium phosphate (Li_3PO_4), are dissolved into the ionic liquid 1-ethyl-3-methylimidazolium trifluoromethanesulfonate through bath sonication. The resulting solution is heated for 1 hour at 250°C in atmosphere using a silicon bath approach. The product, $LiFePO_4$ nanoparticles, is then centrifuged and washed in isopropanol twice, and then washed 3 times with DI water to yield pure $LiFePO_4$ particles. The synthesis process is described briefly in Figure 4 below.

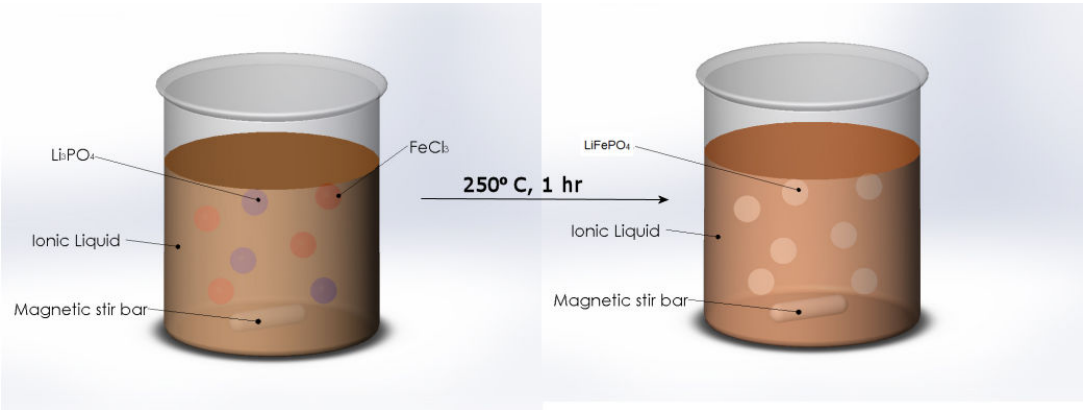

Figure 4: Synthesis mechanism of $LiFePO_4$

Carbonization of the $LiFePO_4$ is conducted through a starch base in conjunction with lithium hydroxide and dihydrogen ammonium phosphate in a

water bath under a nitrogen environment. The synthesis of the carbon matrix occurs at 70°C for 1 hour in a water bath solution contained in a glove box. The carbon coating process is briefly described in Figure 5 below.

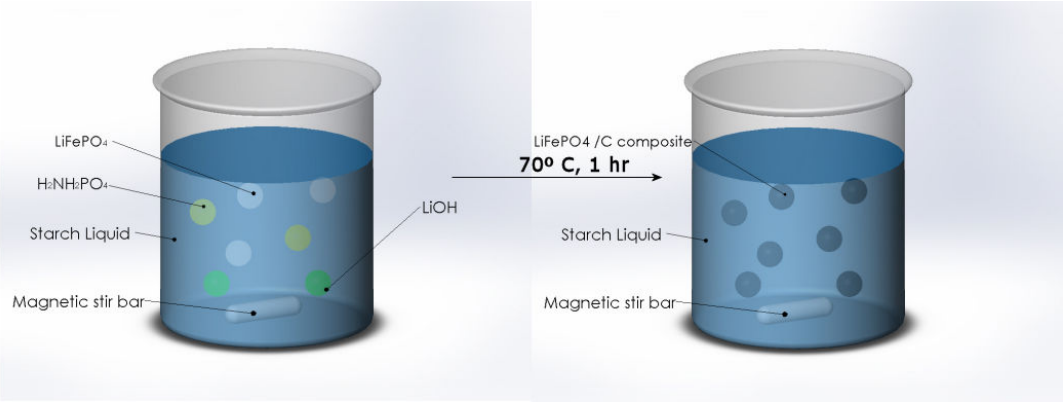

Figure 5: Carbon coating mechanism of $LiFePO_4$

2.3 Experimental

2.3.1 Synthesis of Lithium Iron Phosphate

8 ml of an ionic liquid, 1-ethyl-3-methyl imidazolium trifluroumethanesulfonate (>98% through Sigma Aldrich) is pipetted into a glass reaction vessel. Iron Chloride ($FeCl_3$ > 99% through Sigma Aldridge) and Lithium Phosphate (Li_3PO_4 > 99% through Sigma Aldridge) precursors are added to the glass reaction vessel and sonicated in a bath sonicator for 45 minutes. The solution is placed in a silicon oil bath on top of a digital hotplate with stirring capabilities. A small magnetic stir bar was placed inside the reaction vessel and stirred at 300 RPM. The reaction takes place between 15 minutes to 1 hour, after

which the ionic liquid is placed into micro centrifuge tubes and centrifuged for 15 minutes at 15,000 RPM. Once the product has fully precipitated to the bottom of the micro centrifuge tubes, the supernatant ionic liquid is removed and replaced with isopropanol. This wash is repeated 2 times under the previous centrifuging conditions, and then three more times with DI (de-ionized) water.

2.3.2 Carbon Coating Lithium Iron Phosphate

$LiFePO_4$ nanoparticles were then dispersed into a starch gel containing Li_3PO_4 nanoparticles and dried at 70°C in a water bath. The starch gel was obtained by dispersing 5% by weight of starch into 1 mL of water, $LiFePO_4$ product synthesized in the previous step, and 1M Li3PO_4 (98%> through Sigma Aldrich). The resulting solution was heated in a water bath at 70°C under nitrogen to create a gel. The product material was then sintered at 550°C for 5 hours, under a 1mtorr vacuum. Figure 11 in section 3.2 shows a flow through from the first step to post sintering. Sintering changes the optical color of the product material as well as making the resulting product very brittle.

2.3.3 Characterization of Synthesized Cathode Material

Scanning Electron Microscopy (SEM) and Energy Dispersive X-ray Spectroscopy (EDS or EDX) preparation consists of a standard 3 inch SEM pin being placed into a SEM pin holder. Double sided carbon tape is placed on the SEM pin. A piece of silicon wafer is placed on top of the carbon tape and a small amount of the product solution is drop-casted onto the silicon wafer and allowed

to dry under nitrogen. Images are taken at 5 KeV to obtain the best optical images. EDS spectra are taken at 20 KeV to obtain the most accurate spectrum.

X-ray diffraction was prepared by cutting a microscope grade glass slide into a 1.5 inch square. The product was placed in an aqueous solution for pure nanoparticles and $LiFePO_4$/C was ground finely using a mortar and pestle. Pure nanoparticles were drop-casted directly onto this glass slide and allowed to dry under nitrogen. $LiFePO_4$/C material was placed on a glass slide with clear double sided scotch tape and pressed down with another glass slide to create an evenly distributed surface.

3.0 RESULTS

3.1 Electron Imaging of Nanoparticles

Scanning Electron Microscopy (SEM) reveals the size of particles that are synthesized ionothermally. Synthesizing nanoparticles is advantageous for many reasons, for example high surface area of the material. Traditional bulk materials are very easy to synthesize, but have a low effective surface area which limits the diffusion of lithium ions through the material which in turn decreases performance. Nanoparticles can be placed in a matrix that can further increase the surface area, as well as reducing the strain on the material when a battery charges and discharges.

Shown below in Figures 6-8 are the products resulting from ionothermal synthesis. These particles are very uniform in size and shape covering the entire SEM substrate. However when examining these particles more closely, one notices they are comprised of smaller crystallites which depend on the synthesis conditions. The lower the temperature of the reaction, we notice that there is a conglomeration of smaller crystallites that group together, known as Oswald ripening [99]. It is important to understand the synthesis conditions that result in a more crystalline material. Ideally the more crystalline the material, the better the electrical and ionic conductivity.

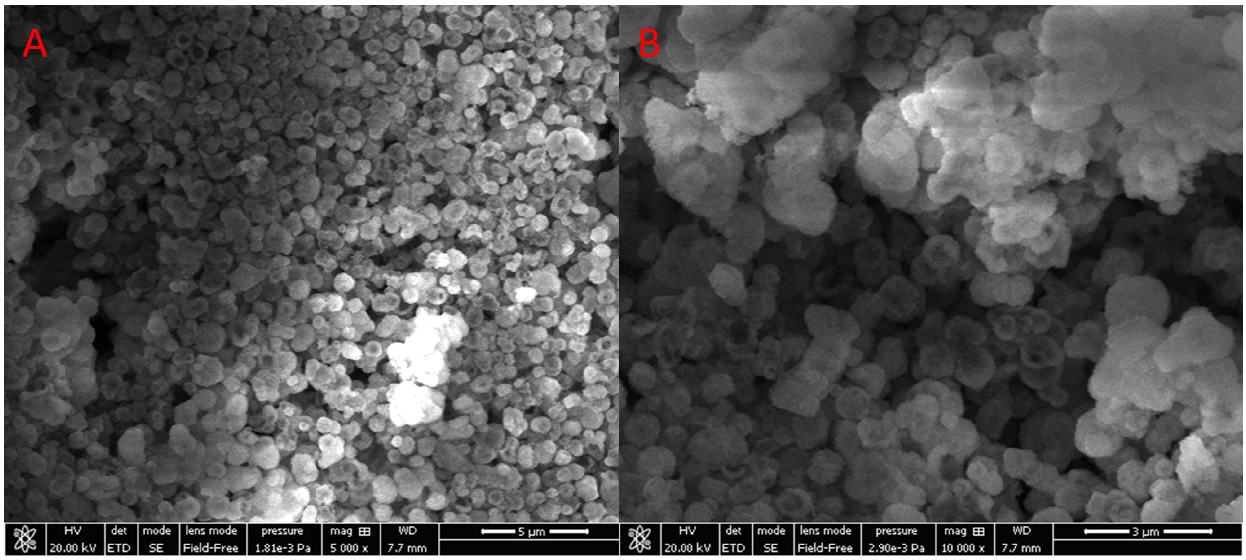

Figure 6: Synthesized $LiFePO_4$ at 250°C using a 2:1 $FeCl_3$:Li_3PO_4 precursor ratio, (A) at 5,000 magnification; (B) at 10,000 magnification.

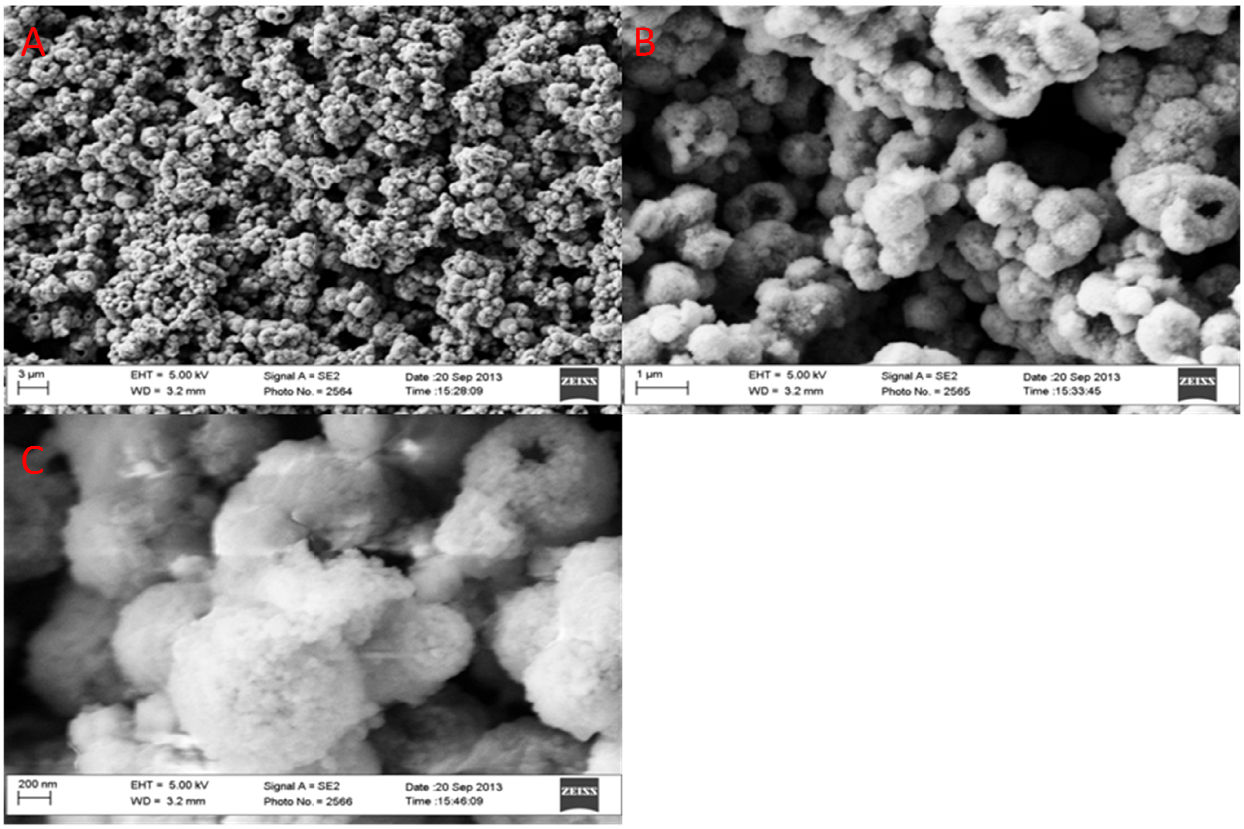

Figure 7: $LiFePO_4$ at 250°C using a 1:1 $FeCL_3$:Li_3PO_4 precursor ratio, (A) at 10,000 magnification; (B) 30,000 magnification; (C) at 400,000 magnification.

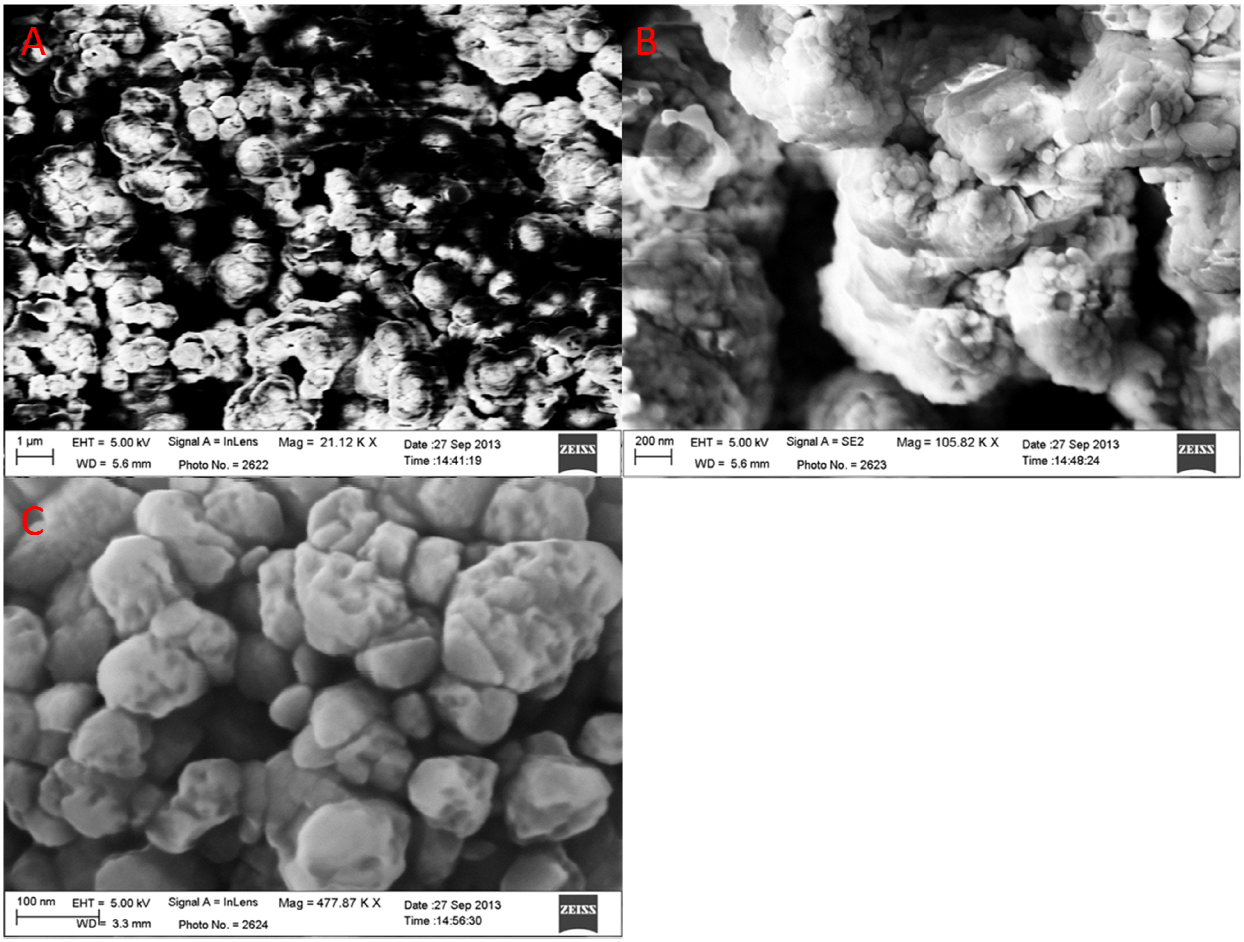

Figure 8: $LiFePO_4$ at 300°C using a 2:1 $FeCl_3$:Li_3PO_4 precursor ratio, (A) 21,120 magnification; (B) 105,820 magnification; (C) 477,870 magnification.

3.2 Carbon Coating Process

Multiple experiments were conducted to determine the correct molar ratio of $LiFePO_4$ to starch to obtain the least amount of starch by weight. The formation of a carbon matrix is extremely important to improve both the specific capacity and the cycle performance of $LiFePO_4$., however too much carbon in the matrix will inhibit Li ion diffusion decreasing performance. Experiments show that the minimal amount of carbon to induce gelling is 0.25 mol/L (Molar), shown in

Figure 9. All molar ratios greater than 1 M showed formation of a sol-gel, however the excessive weight percentage of carbon hinders electrochemical performance.

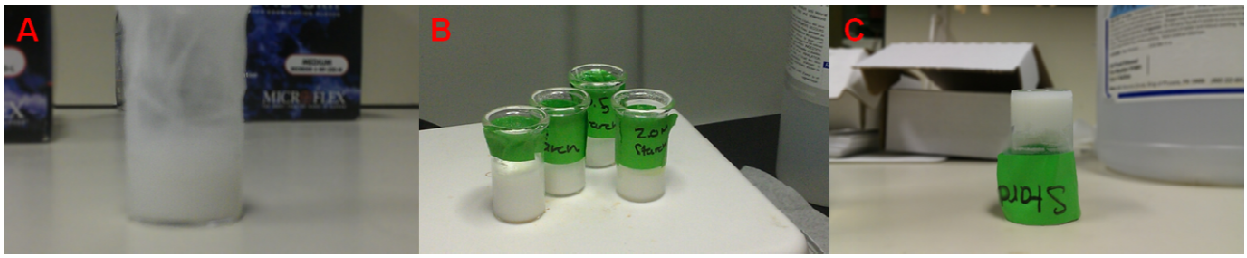

Figure 9: (A) starch/Li_3PO_4 solution pre-synthesis; (B) starch/Li_3PO_4 solution during synthesis of sol-gel; (C) starch/Li_3PO_4 solution sol-gel post synthesis.

Once a minimum Molar sol-gel solution has been obtained, we have then investigated the effect of adding $LiFePO_4$ nanoparticles to the solution. Shown in Figure 10, the synthesized nanoparticles become well integrated and dispersed into the sol-gel solution after 15 minutes of sonication. The objective of the carbon coating of nanoparticles is to create a matrix where electrons can flow from the electrode to the current collector without hindering Li^+ diffusion. Confirming that the nanoparticles are well dispersed into the sol-gel allows for more surface area of $LiFePO_4$ to be exposed while maintaining high electrical conductivity. For practical reasons, the limiting factor in each carbon coating experiment has been $LiFePO_4$ and has been determined that adding 0.5 g of $LiFePO_4$ to 0.025 g of starch results in approximately 4.8 g of carbon coated material. The total weight of the product is reduced due to the fact that some material cannot be removed from the walls of the glass reaction vessel.

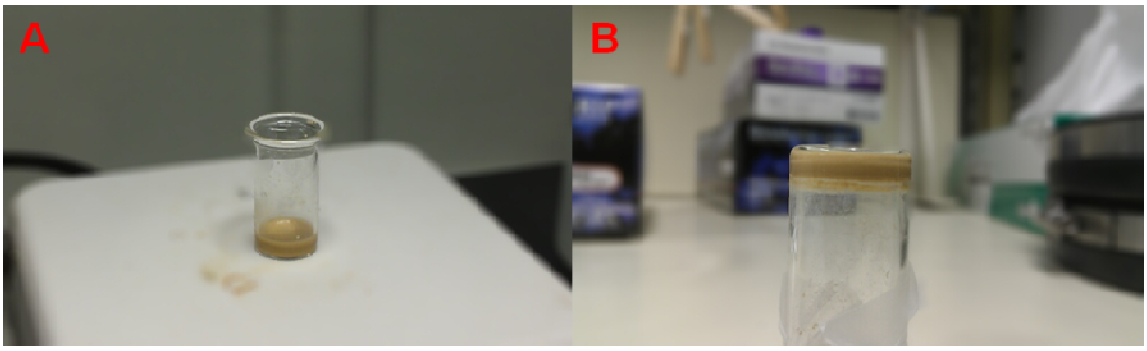

Figure 10: (A) Synthesis of starch sol-gel with integrated $LiFePO_4$ nanoparticles; (B) post synthesis of sol-gel.

Annealing the sol-gel, called carbonization, is the final step of creating a working electrode material. The sol-gel material is placed in a quartz boat and placed in a CVD (chemical vapor deposition) furnace shown in Figure 11. A vacuum furnace is also acceptable to use for this process, but the availability of a CVD furnace in our lab makes this process possible. Once the boat is secured in the CVD, a 1 mtorr vacuum evacuates the tube in the furnace. High purity nitrogen is then pumped into the furnace which inhibits the oxidation of carbon and $LiFePO_4$ during synthesis.

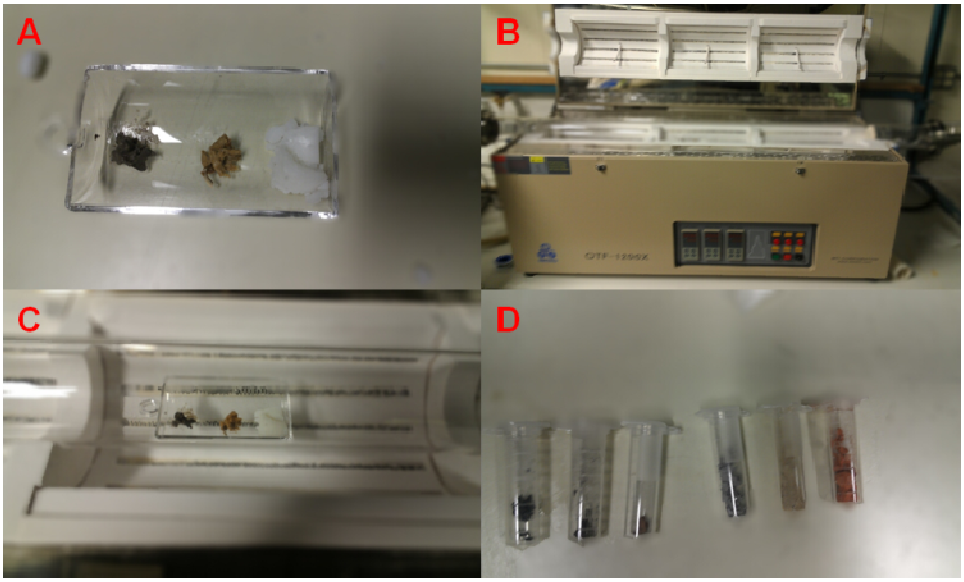

Figure 11: (A) Sol-gel product placed in a quartz boat; (B) CVD furnace used in carbonization; (C) quartz boat with product in CVD furnace; (D) Carbonized material, the left three tubes synthesized for 550°C for 2 hours and the right three tubes synthesized at 550°C for 5 hours.

Characterization of the $LiFePO_4$/C material has been conducted to confirm the carbonization process has coated the nanoparticles evenly. SEM images have been taken shown in Figure 12 to confirm the effectiveness of the carbonization process which does not affect the particle size of $LiFePO_4$. As you can see in Figure 12B, the nanoparticles size still ranges from 400nm to 4µm which can be attributed to the inability to use a ball mill. Grinding the particles before the carbon coating process will increase the surface area of the synthesized particles and allow for more distributed coating of carbon. We also predict that the increase in surface area will enhance the Li^+ diffusion through the

crystal structure which will in turn increase the electrochemical performance of the cathode material.

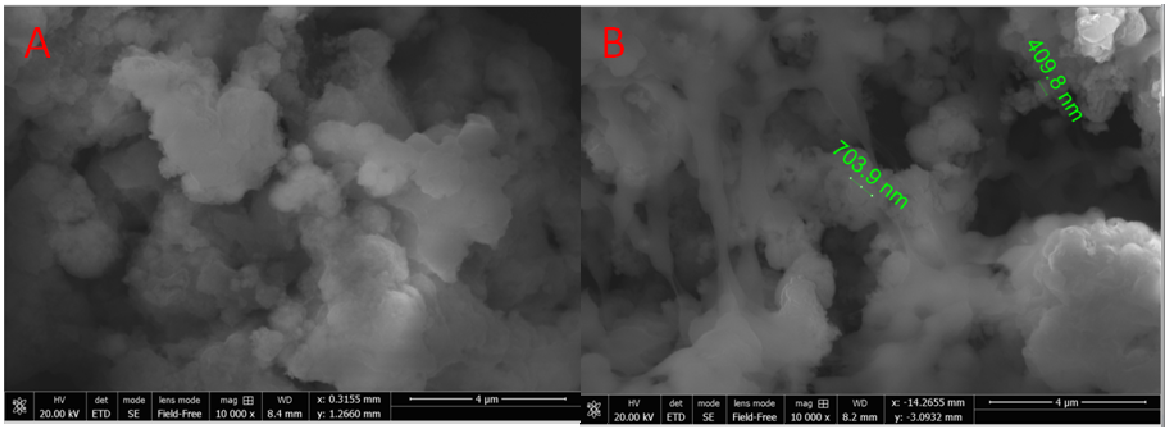

Figure 12: (A) synthesized $LiFePO_4$; (B) carbon coated $LiFePO_4$

3.3 Energy Dispersive X-Ray Spectroscopy

3.3.1 Temperature Dependence on Synthesis

Once nanoparticles have been synthesized and imaged, we have investigated the elemental composition of these nanoparticles using Electron Dispersive X-ray Spectroscopy (EDS or EDX). Many synthesis conditions have been observed given in Tables 1-6, however one particular set of synthesis conditions yield very interesting results. When our reaction takes place at 250°C with a precursor ratio of 2:1 Li_3PO_4:$FeCl_3$ at a 0.1 Molarity for one hour, we notice that the products are in the correct ratio, shown in Figure 1. The chemical formula for lithium iron phosphate is $LiFePO_4$, and we can see that Fe, P, and O are in approximately the correct ratio to the chemical formula of $LiFePO_4$.

Element	Wt %	Wt % Sigma	Atomic %
O	39.68	0.068	64.55
P	19.62	0.43	16.48
Fe	40.7	0.67	18.97

Table 1: EDS analysis of Synthesized $LiFePO_4$ at 250°C using a 2:1 $FeCl_3$:Li_3PO_4 precursor ratio.

With regard to $LiFePO_4$ synthesis, three main conditions shape the formation of a high performing material: temperature, molar ratio, and total mols of the solution. The most obvious and extremely important factor in the formation of $LiFePO_4$ is temperature. Experiments have been conducted to optimize the intercalation of iron into the crystal structure of our product. Temperature experiments have been run at 200, 220, 230, 240, 250, 270, and 280°C, while holding molar ratios and Molarity constant, to determine the effect on our system. All experiments were run multiple times to verify the validity of the data collected. After synthesis, SEM and EDS were conducted to determine the atomic composition of the product. Shown in Tables 2-5, a clear trend has been observed, that increasing the temperature of the reaction allows for greater iron intercalation into the product's crystal structure. In order to obtain pure $LiFePO_4$ product we must verify that the atomic percentage of iron to phosphorous is in a 1:1 ratio as well as confirming the crystal structure through XRD. A balance of

temperature in conjunction with other synthesis conditions has been obtained in order to create a working cathode material.

A	$LiFePO_4$ Synthesis @ 2:1 Fe:P Ratio		
Element	Atomic % @ 240°C	Atomic % @ 250°C	Atomic % @ 270°C
O	71.80	62.30	60.24
P	7.85	16.89	12.12
Fe	7.68	20.81	17.84

Table 2: Effect of Temperature using a 2:1 $FeCl_3$:Li_3PO_4 precursor ratio of cathode product.

B	$LiFePO_4$ Synthesis @ 1:2 Fe:P Ratio		
Element	Atomic % @ 200°C	Atomic % @ 220°C	Atomic % @ 250°C
O	74.95	70.79	69.29
P	16.79	14.12	20.00
Fe	3.91	7.57	10.71

Table 3: Effect of Temperature using a 1:2 $FeCl_3$:Li_3PO_4 precursor ratio of cathode product.

C	$LiFePO_4$ Synthesis @ 1:1 Fe:P Ratio		
Element	Atomic % @ 230°C	Atomic % @ 250°C	Atomic % @ 270°C
O	73.29	67.93	73.31
P	13.88	13.22	12.80
Fe	5.63	6.83	6.54

Table 4: Effect of Temperature using a 1:1 $FeCl_3$:Li_3PO_4 precursor ratio of cathode product.

Although the exact temperatures in Tables 2-4 are not exactly matching, the objective of each of these 9 types of experiments was to observe the temperature effect on iron intercalation into the cathode crystal structure. We observe that the amount of iron that is present within the cathode's crystal structure increases with the increase of temperature provided to the reaction.

3.3.2. Precursor Ratio Dependence on Synthesis

Molar ratios of precursors have been investigated to determine the effect on the product synthesized. Ratios consisting of 1:1, 1:2, and 2:1 with respect to the precursors Li_3PO_4: $FeCl_3$ were synthesized at different temperatures and total mol conditions. Shown in Table 5, the percentage of iron is greatly influenced by the molar ratios of precursors in the final product. When synthesis of higher or equal Li_3PO_4 concentrations is observed, phosphorous concentrations are about twice as large as iron on average. When the concentration of $FeCl_3$ is larger than the concentration of Li_3PO_4, the iron percentage is greatly increased.

$LiFePO_4$ Synthesis @ 250°C			
Element	1:1 Fe:P Atomic %	1:2 Fe:P Atomic %	2:1 Fe:P Atomic %
O	67.93	69.29	62.30
P	13.22	20.00	16.89
Fe	6.83	10.71	20.81

Table 5: Effect of precursor ratio on cathode product synthesized at 250°C.

3.3.3. Molar Ratio Dependence on Synthesis

Optimization of all facets of this project is necessary in order to create a sustainable and cost effective method to produce high performance cathode material for industrial use. On the laboratory bench scale, the amount of ionic liquid used in each reaction is not a large economic factor. However since our synthesis method is geared towards an industrial application, a method to reduce all waste has been investigated. The solution for increasing the amount of product per unit time, as well as cutting down waste of ionic liquid, has been to increase the total mol concentration of precursor for each experiment. Early experiments consisted of varying temperature and molar ratio of precursor using a 0.1 M total solution showed very promising results in $LiFePO_4$ formation. However the product generated was in the few mg regime, which wasted much ionic liquid. Therefore experiments were conducted at 0.5M and 1M to see the effect on the resulting product. Shown in Table 6 are EDS computations showing that increased Molarity of precursors, while keeping temperature and precursor ratios constant, result in a reduction of iron intercalation. The solution to

incorporate more iron into the crystal structure of our product has been to increase the thermal energy to obtain a 1:1:4 ratio of Fe: P: O. For example when 250°C was necessary in the formation of $LiFePO_4$ at 0.1M, a higher temperature will be needed at 1M to obtain a comparable product.

Synthesis of LiFePO4 at 250C using a 2:1 FeCl3:Li3PO4 precursor ratio			
Element	Atomic % @ 0.1M	Atomic % @ 0.5M	Atomic % @ 1M
O	62.3	67.46	71.51
P	16.89	13	10.03
Fe	20.81	10.21	5.88

Table 6: Effect of molar ratio on composition of synthesized material @ 250°C at a 2:1 $FeCl_3$:Li_3PO_4 precursor ratio

3.4 X-ray Diffraction Data

Correctly identifying which synthesis conditions yields the best product cannot however be done solely with one type of characterization. EDS can analyze elements with large atomic numbers, but struggle to identify elements like hydrogen, helium, and lithium. A problem of EDS analysis of $LiFePO_4$ is that $FePO_4$ can be a side product of the reaction and one would not be able to differentiated between the two compounds solely using this method.

To fully characterize $LiFePO_4$, other methods must be conducted to confirm that $LiFePO_4$ has been synthesized instead of byproducts. One such method of analyzing a particular material is X-ray Diffraction (XRD). This method

can tell us the crystal structure by obtaining the reflection and refraction of X-rays from the material at different angles relative to the sample. Each crystalline material has a particular pattern of peaks when X-rays bombard the sample at a certain angle, which are like finger prints used to identify each compound.

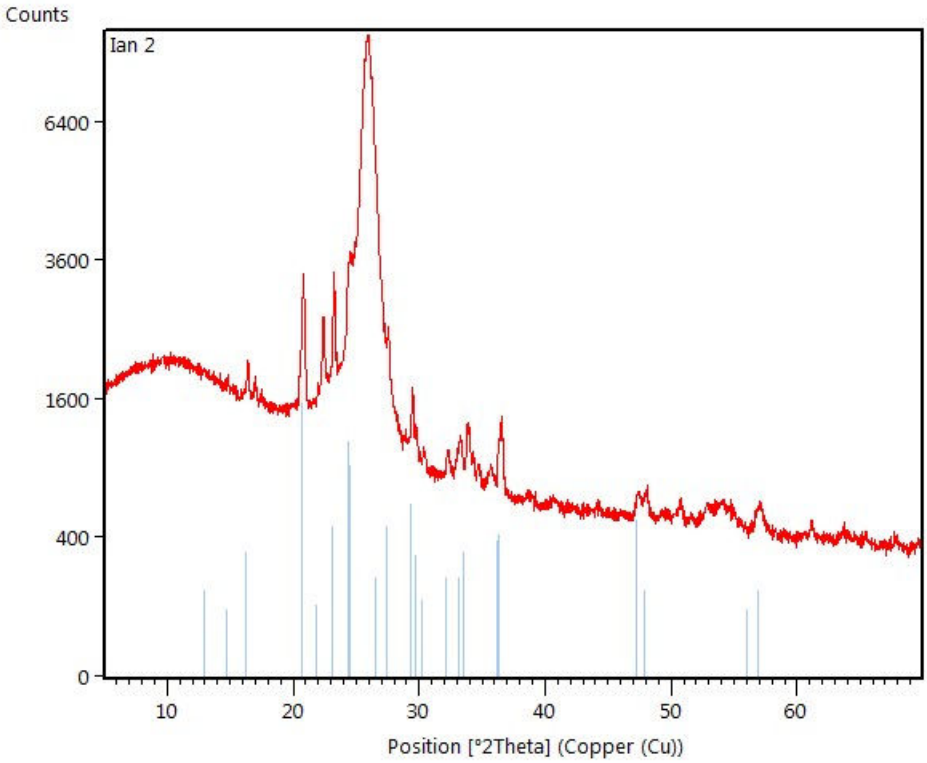

Figure 13: XRD plot of product synthesized at 250°C with a precursor ratio of 2:1 $FeCl_3$:Li_3PO_4

Figure 13 shows the XRD results from synthesized nanoparticles at 250°C with a precursor ratio of 2:1 $FeCl_3$:Li_3PO_4 without any further post-treatment. The red graph indicate the XRD plot of our synthesized material and the blue graph

indicates a literature source that matches well through the XRD database [103]. Our plot matches very well with unstoicheometric lithium iron phosphate ($Li_3Fe_2(PO_4)_3$) which indicates that the ionothermal synthesis by itself would not yield $LiFePO_4$.Crystallinity is also an issue as we can see that there are broad peaks throughout the sample, where more crystalline material would yield very sharp peaks.

Therefore XRD data was taken for our carbon coated/sintered material to observe the effects that heat treatment post synthesis plays in the role of the crystal structure of the material. Shown in Figure 14 is the same material shown in Figure 13 except for the fact that it was carbon coated with 20% preloaded starch and sintered to 550°C. We observed that the peaks in Figure 14 are much sharper than in Figure 13 which could indicate better crystallinity. Also this material matches up with $LiFePO_4$ found in the XRD database which indicates that heat treatment plays a large role in the formation of crystalline $LiFePO_4$ [109]. Although the database XRD and our XRD plot match well, some 2θ peaks are shifted slightly and some peaks are not as intense as we would like. Future studies should be conducted to determine at which temperature the resulting $LiFePO_4$ has the best crystallinity for optimal electrochemical performance.

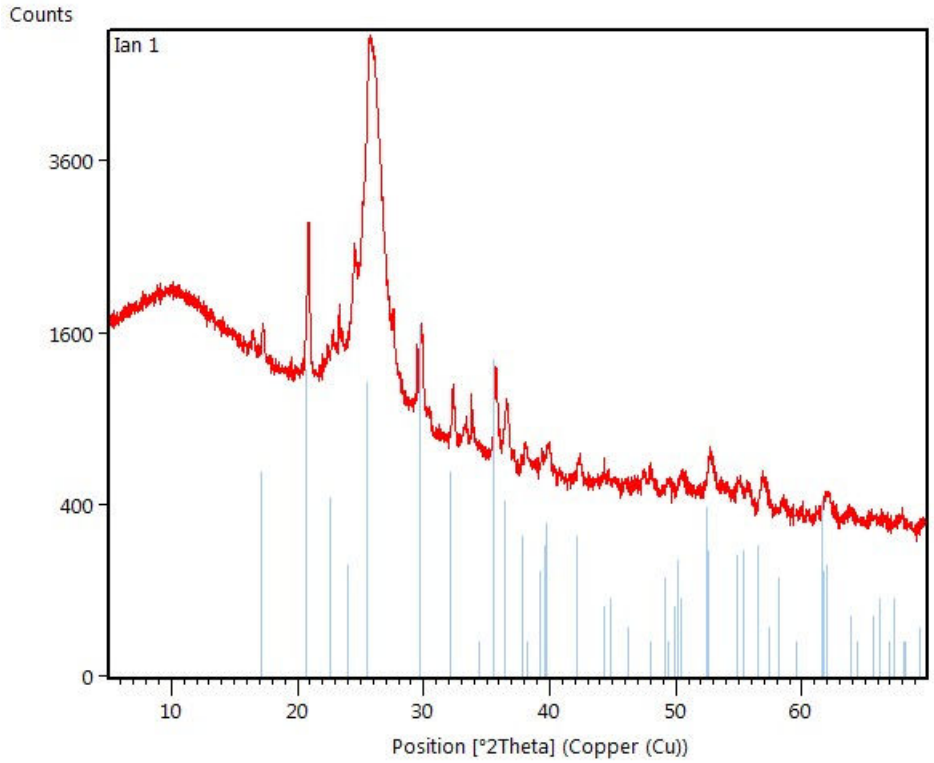

Figure 14: XRD plot of carbon coated and sintered $LiFePO_4$

Through rigorous experimentation using varying synthesis conditions, we have concluded that the formation of a phosphor-oxide structure is a side reaction to the synthesis of $LiFePO_4$. Once enough energy in the form of temperature, as well as the increased concentration of $FeCl_3$ precursor is provided, iron intercalation into the crystal structure yields the desired $LiFePO_4$ cathode material. The proposed mechanism for the synthesis of pure $LiFePO_4$ is shown in equation one below:

$$2FeCl_3(s) + 2Li_3PO_4(s) \xrightarrow{\Delta} 2LiFePO_4(s) + Cl_2(g) + 4\,LiCl$$

Conducting EDS explained above does not detect the presence of chlorine within the $LiFePO_4$ nanoparticles. If our proposed mechanism is correct, then the LiCl generated in the reaction does not precipitate out of the ionic liquid post synthesis. To test that there is chlorine present in the ionic liquid, silver nitrate ($AgNO_3$) is added to a mixture of ionic liquid post synthesis and water to detect the presence of chlorine anions. Shown in Figure 15 below, is an image of precipitate forming when $AgNO_3$ is introduced to the ionic liquid/water solution. This white precipitate is AgCl, which confirms the presence of Cl^- anions dissolved in the ionic liquid, which ultimately proves the proposed mechanism for the formation of $LiFePO_4$.

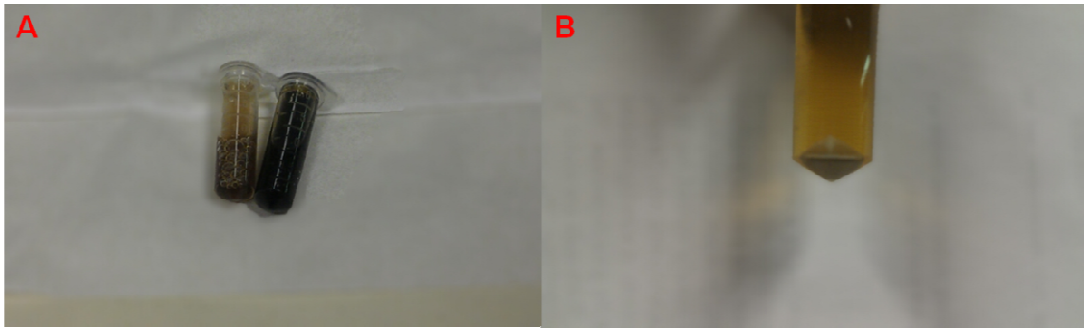

Figure 15: (A) Left an image of ionic liquid/water solution, right an image of pure ionic liquid both post synthesis; (B) precipitant formed after introducing $AgNO_3$ to aqueous ionic liquid solution.

3.5 Electrochemical performance of synthesized cathode material.

Coin cell testing will determine the cycle performance of our cathode material at different charge/discharge rates. Both the specific capacity and the

cycle life of our cathode material will be determined through this method. The standard rate for cycling is noted by the letter C, in which the battery is fully charged from a starting potential to an end potential in one hour. An example would be if a cell phone had no charge to power the device, a 1C rate would fully charge the battery in 1 hour. Consequently a 2C rate can charge a battery in 30 minutes; a 10C rate can charge a battery in 6 minutes and so on. Cycle performance in a device is vital to determine the lifespan of the battery and also the optimal time in which the battery can charge or discharge. Quicker charge and discharge of a battery would be very beneficial in many applications, but inherent problems arise when using fast C rates. Charging and discharging an electrode creates a mechanical strain on the material and if cycled too quickly, catastrophic failure of the electrode can occur creating irreversible damage [102, 103].

Conducting cyclic testing experiments begins with placing the desired material into a coin cell. Our $LiFePO_4$/C composite is placed in a solution of 1-methyl-2pyrrolidinone (> 99.5% purity, Fisher Scientific) containing 5% by weight of polyvinylidene fluoride (>98%, Fisher Scientific). This paste containing our cathode product is spread over the aluminum current collector in a glove box filled with argon. The material is placed in a coin cell cap with the current collector facing the back of the case, and then an electrolyte ($LiPF_6$) is drop-casted onto the cathode. A separator is then laid on top of the cathode and a spring and a spacer are placed on top of this layer. Then an anode material, in

our case a half cell is used which incorporates lithium foil as our anode, is placed over the separator and is sealed with an end cap in a hydraulic press. The coin cell is then transferred to an Arbin coin cell tester where the experiment is conducted.

Cyclic testing using the Arbin tester, located in the Winston Chung Global Energy Center, has confirmed that we have synthesized active cathode material that can be used in a lithium ion battery. Shown in Figure 16, we can see that the cathode material charges and discharges at a very uniform rate that creates minimal capacity loss over time.

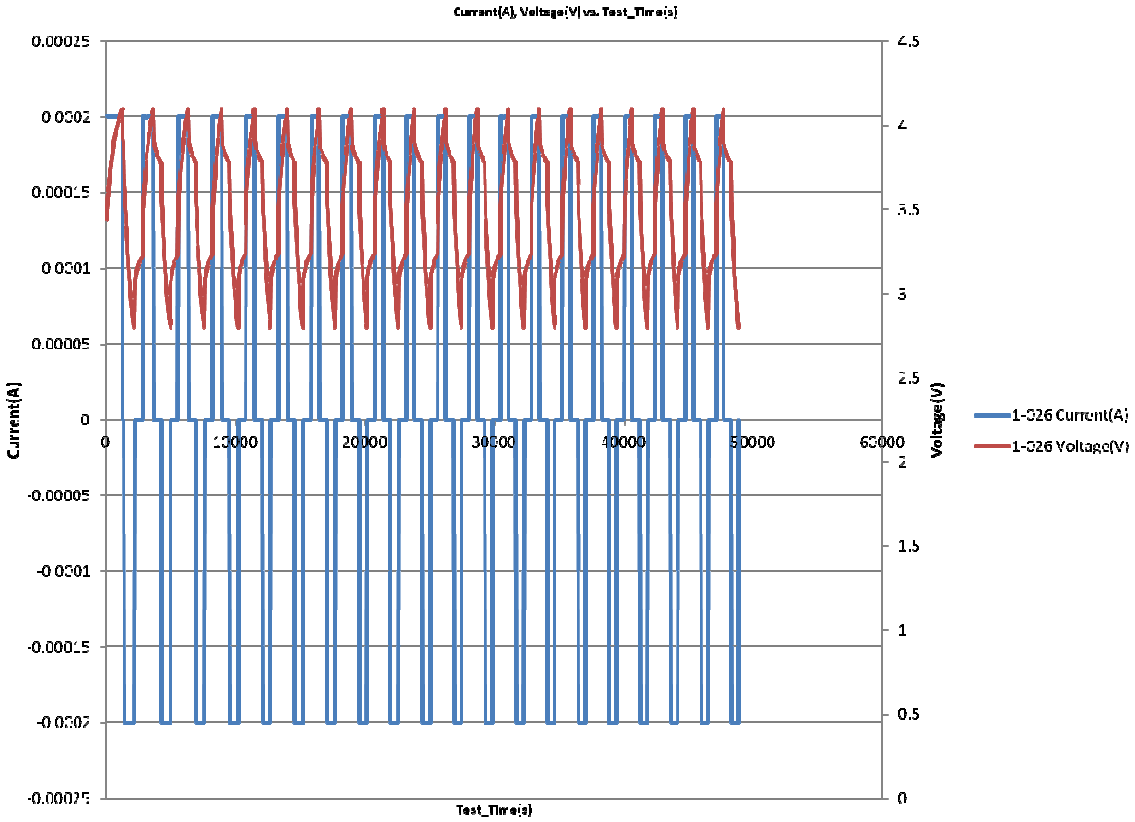

Figure 16: Cycle performance of synthesized $LiFePO_4$ at a 3C rating.

Figure 16 illustrates the charging and discharging characteristics of our cathode material, where the blue line indicates current in A, and the red line indicates the potential V. This cathode was cycled 20 times, a charged and discharge is considered 1 cycle, and the total capacity was observed for each cycle. The highest capacity was recorded during the first cycle and the last cycle recorded the lowest total capacity which is consistent with previous results from Jianxin Zhu et al. This is most likely due to the inability of full lithium ion intercalation into the crystal structure during discharge. This phenomenon

intensifies when the charge/discharge rate is increased. Figure 16 illustrates the loss in capacity over cycles, but ultimately reaches a stable total capacity.

A 1C experiment was also conducted on our $LiFePO_4$ material to determine the total capacity of the cathode at different charge/discharge rates. As shown in Figure 17, the charge and discharge potentials are very stable with minimal capacity loss over cycles. We calculate the specific capacity, the ability for a certain material to hold a charge, to be 155mAh/g on the first charge. By the 6^{th} cycle, the capacity drops to 123 mAh/g but is relatively stable after the 5^{th} cycle. A comparison between the charge rate and the specific capacity of the material is shown in Figure 18. It is observed that the slower the charge and discharge rates, the more total charge the cathode can hold. The maximum specific capacity observed at a 1C rate is 155 mAh/g compared to 112 mAh/g for a 3C discharge rate. Both of these cathodes exhibit a loss of capacity over cycles, but stabilize or have a reliably predictable capacity after 5 cycles.

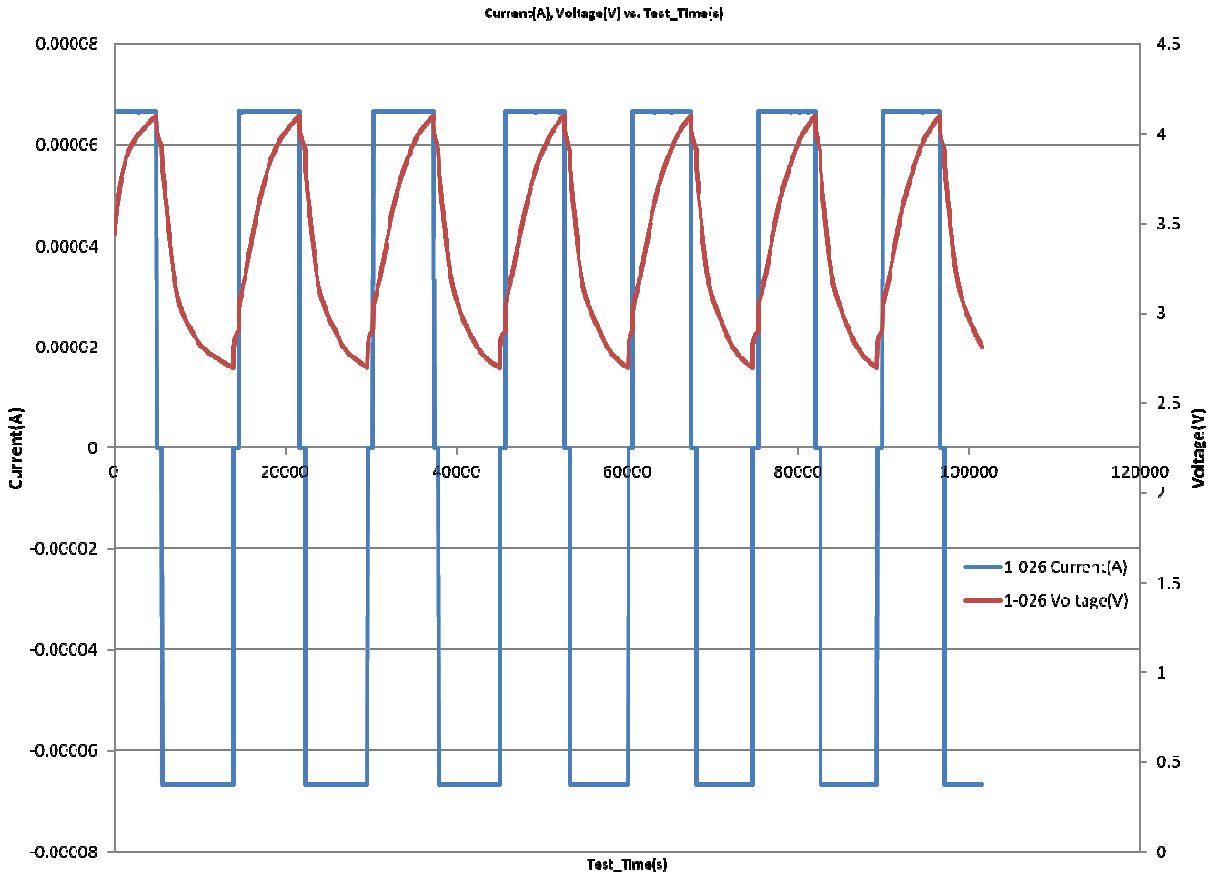

Figure 17: Charge/Discharge curve of $LiFePO_4$ at a 1C discharge rate

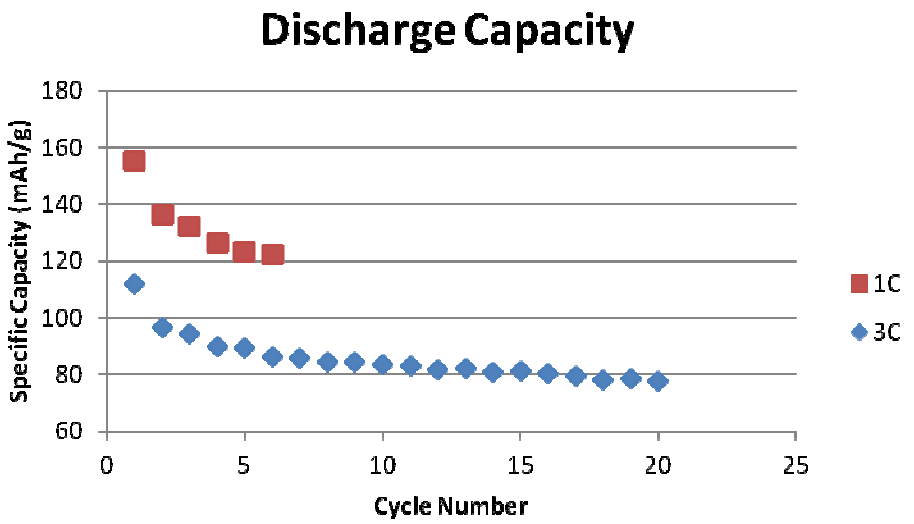

Figure 18: Capacity comparison between different discharge rates.

Electrochemical data was also compared between synthesized $LiFePO_4$ and carbon coated $LiFePO_4$ to determine the impact carbon plays on the performance of $LiFePO_4$. Both carbon coated and uncoated $LiFePO_4$ sample do contain carbon, however the carbon coated sample was heat treated with starch at 550°C for 5 hours and the untreated $LiFePO_4$ was mixed with polypyrrole doped with carbon black during the preparation of the cathode. Shown in Figures 19 and 20 are the electrochemical results of uncoated and coated $LiFePO_4$ nanoparticles. Although these cathodes had charged well enough, the experiment resulted in a catastrophic failure of the material due to the fact we charged the cathode past the voltage limit of our $LiFePO_4$ material. The reason for overcharging was to get the most charge out of our material as possible. One reason why we believe this battery has catastrophically failed is due to the fact

that the voltage slowly starts do decrease (after 4.23 V and 4.28 V for Figure 19 and 20 respectively) even though positive current is being passed through the device. We then manually discharged the battery to see if the cathode could be cycled more than one time, but the cathode could not be charged again. If more time was given, we would extensively review the difference between carbon coated and non coated nanoparticles at different carbon precursor percentages and the effect this would have on the electrochemical properties of our cathode material.

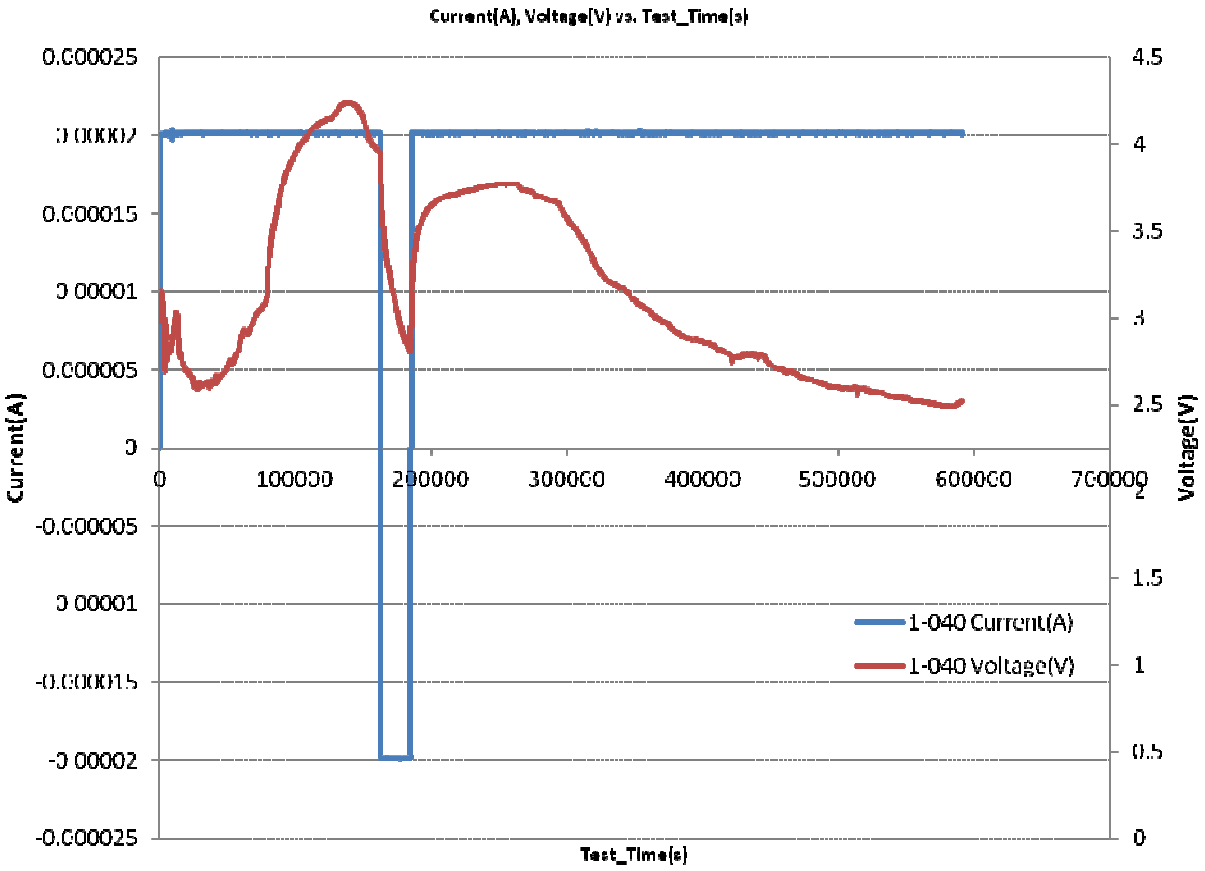

Figure 19: Charge/discharge curve of non-coated $LiFePO_4$

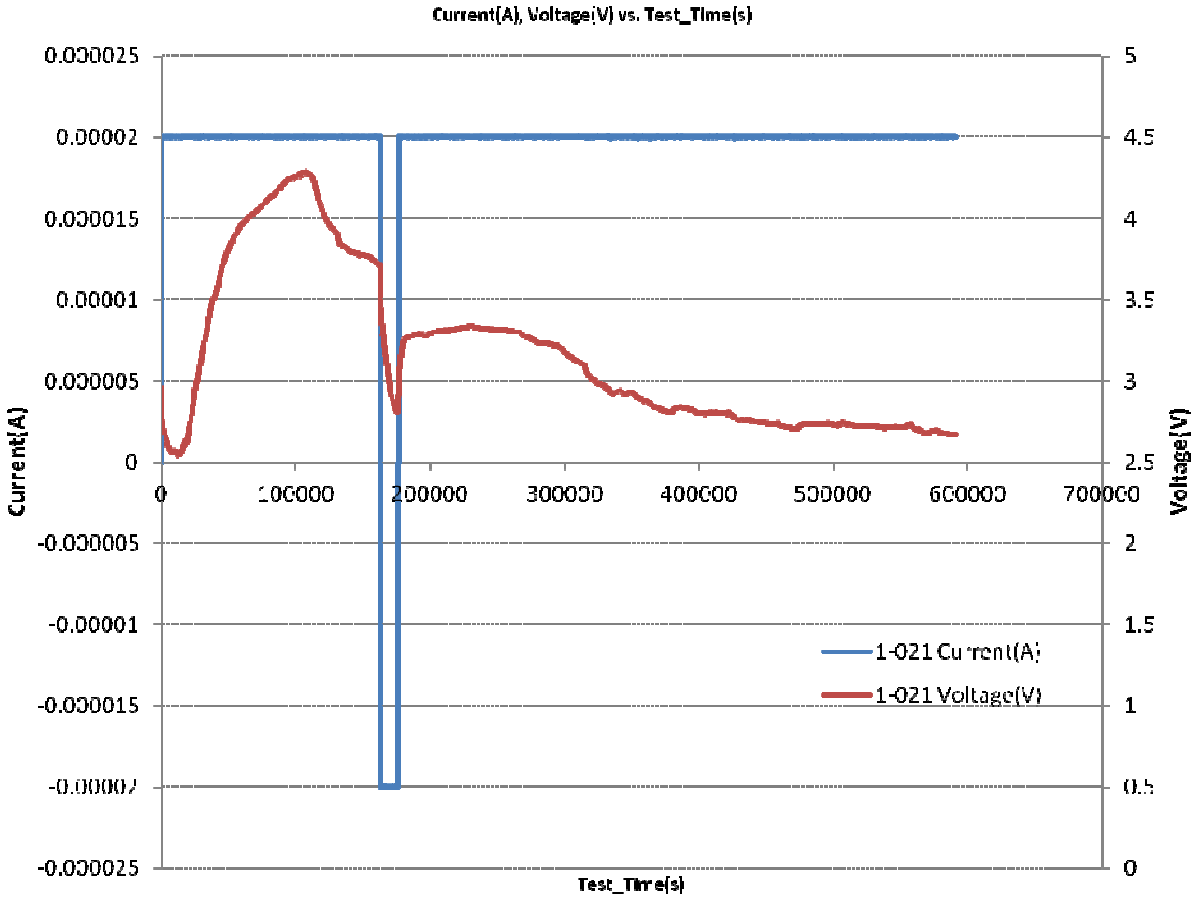

Figure 20: Charge/discharge curve of carbon coated $LiFePO_4$.

4.0 Conclusion

An affordable yet high performance $LiFePO_4$/C cathode material has been synthesized through an ionothermal approach. The incorporation of the ionic liquid 1-ehtyl-3-methylimidazolium trifluoromethanesulfonate in a bath synthesis with iron chloride and lithium phosphate as precursors has allowed for the precipitation of crystalline $LiFePO_4$ using significantly less temperature and less time than previous methods. Ionothermal synthesis route has enabled the precipitation of $LiFePO_4$ in one hour in comparison to 3-24 hours in previous synthesis methods such as solid-state and solvothermal reactions.

Figures 8, Figure 14, and Table 2 shows nanoparticles between the ranges of 200-400 nm in diameter that have been precipitated that have correct atomic ratios and are in the correct crystal structure. The reduction of energy, time, and the scalability of our process used in the production of this cathode material has decreased the manufacturing cost which will benefit the battery industry greatly. Timeline and further temperature studies should be carried out with regards to crystal morphology.

In addition, the incorporation of a Li/C matrix onto the $LiFePO_4$ nanoparticles have been synthesized shown in Figure 12. Also, Figure 14 shows that the crystal structure of $LiFePO_4$ is not impacted by the carbonization process. Further investigation into the effect that carbon coating has on the effect of total capacity and mechanical stability of the cathode is necessary. These

experiments are currently being investigated; however time constraints have hindered the reporting of this data on my thesis.

5.0 Future Work

During this project we have proven that electrochemically active $LiFePO_4$/C cathode material can be synthesized ionothermally in a timely fashion. However the material has yet to reach a specific capacity at or near the theoretical limit of this material which is 170 mAh/g. Increasing the surface area by creating a meso-porous composite structure, and/or reducing the particle size of the cathode material, are critical to increasing the capacity of our product. In turn these methods would also increase the energy density of the material, allowing the potential of applications in which this material is used would skyrocket.

The main contribution of this project was to create an affordable high performance cathode material that has the potential for scale up production in industry. Though the actual synthesis is straight forward and simple, the limiting competitive factor remains the cost of production. Currently the cost limiting factor of production is the ionic liquid medium used to facilitate the reaction. To further reduce costs, making this production method highly valuable, the amount of ionic liquid used needs to be reduced or recovered.

We have shown that $LiFePO_4$/C cathode material can be made through optimizing temperature and precursor ratio at a 0.1 M total ratio. However this molar ratio can be increased in order to reduce the amount of ionic liquid needed per unit gram of product. However the increase of molar concentration means

that temperature has to be precisely controlled to obtain the optimal cathode material.

A long term solution of reducing the amount of ionic liquid is to reuse the post synthesized slurry. This method would include separating the ionic liquid from the precipitated product, which has been shown previously in this paper, and then separating the free Li and Cl ions that are dissolved in the solution post synthesis. Although this method is very time and energy intensive, it has the greatest upside to reduce long term cost by reducing the overall amount of ionic liquid needed to be purchased and used per unit gram of product. Possible methods to increase the purity of ionic liquids include ion chromatography and electrochemical separation.

6.0 References Cited

[1] Riskin, J. University of California Press, 1998. Historical Studies in the Physical and Biological Sciences, Vol. 28, No. 2 pp. 301-336

[2] Frood, Arran "Riddle of 'Baghdad's Batteries." BBC News. (2003-02-27).

[3] Corder, G. Journal of Virginia Science Education, pp 33-36 (2006).

[4] Brain, Marshall, B.; Charles, W.; Pumphrey, B.; and Pumphrey, C. How Batteries Work. <http://electronics.howstuffworks.com/everyday-tech/battery1.htm> 2013.

[5] Padhi, A.K.; Nanjundaswamy, K.S.; Goodenough, J.B. (1997) Journal of the Electrochemical Society. 144(4):1188.

[6] Barak, M. Institution of Electrical Engineers (1980).

[7] Wang, B.; Bates, J.B.; Hart, F. X.; Sales, B.C.; Zuhr, R.A.; Robertson, J.D. Journal of the Electrochemical Society, 1996. 143(10): P. 3203-3213

[8] Poizot, P.; Laruelle, S.; Grugeon, S.; Dupont, L.; Tarascon, J.M. Nature, 2009. 407(6803): P. 496-499

[9] Gummow, R.J.; Thackeray, M.M. Electrochemical Society Inc., 1994. 141(5): P 1178-1182

[10] Dekock, P.C. Annals of Botany, 1956. 20(1): P. 133-141.

[11] Bazzi, K.; Dhindsa, K.; Dixit, A.; Sahana, M.B.; Sudakar, C.; Nazri, M.; Zhou, Z.; Zhou, P.; Naik, V.; Nazri, G.; Naik, R. J. Mater. Res., Vol. 27, No. 2, Jan 28, 2012.

[12] Barton, J.P.; Infield, D.G. IEEE Transactions on Energy Conversion, (2004).

[13] Nagaura, T. Progress in Batteries and Solar Cells, 10 (1991) 209–226.

[14] Gummow, R.J.; Dekock, A.; Thackeray, M.M. Solid State Ionics, (1994).

[15] Dekock, P.C. Annals of Botany, Pg. 133-141. (1956).

[16] Andrea, D. Battery Management Systems for Large Lithium-Ion Battery Pack, Pg. 9. (2010).

[17] McMichael, F.C.; Henderson, C.; Spectrum, IEEE. (1998).

[18] MSDS: LITHIUM-ION BATTERIES. National Power Corporation, (2004).

[19] Henry, J.; Heinke, G. Environmental Science and Engineering; Prentice Hall, (1996).

[20] Edmonds, J.; Reiley, J.M. Global energy - assessing the future. (1985).

[21] Poizot, P.; Laruelle, S.; Grugeon,S.; Dupont, L.; Tarascon, J.M. Nature, (2000).

[22] Chen, L.; Shet, S.; Tang, H.; Wang, H.; Deutsch, T.; Yan, Y.; Turner, J.; Al-Jassim, M. Journal of Materials Chemistry, (2010).

[23] Installed tomorrow

[24] Monahov, B.; Pavlov, D.; Kirchev, A.; Vasilev, S. Journal of Power Sources, 113 (2003). 281.

[25] Pavlov, D.; Kirchev, A.; Stoycheva, M.; Monahov, B. Journal of Power Sources, 137(2004) 288.

[26] Takehara, Z.; Kanamura, K. Journal of the Electrochemical Society, 134 (1987) 13.

[27] Salameh, Z.M.; Casacca, M.A.; Lynch, W.A. IEEE Transactions on Energy Conversion, Vol. 7, No.1, March 1992

[28] Rosseinsky, D.R.; Mortimer, R.J. Adv. Mater. 2001, 13, 783 – 7

[29] Wang, B.; Bates, J.B.; Hart, F. X.; Sales, B.C.; Zuhr, R.A.; Robertson, J.D. Journal of the Electrochemical Society, 1996. 143(10): P. 3203-3213

[30] Poizot, P.; Laruelle, S.; Grugeon, S.; Dupont, L.; Tarascon, J.M. Nature, 2009. 407(6803): P. 496-499

[31] Whitingham, M.S. Science, 11 June 1976: Vol. 192 no. 4244 pp. 1126-1127.

[32] [U.S Patent # 4,302,518]

[33] [Panasonic data sheet]

[34] Whittingham, M.S. Progress in Solid State Chemistry, 12, 41-111

[35] Kjeldsen, P.; Barlaz, M.A.; Rooker, A.P.; Baun, A.; Ledin, A.; Christensen, H. Present and Long-Term Composition of MSW Landfill Leachate: A Review, Critical Reviews in Environmental Science and Technology, (2002). 32(4): P. 297-336

[36] Andrea, D. Battery Management Systems for Large Lithium-Ion Battery Pack, Pg. 9. (2010).

[37] McMichael, F.C.; Henderson, C.; Spectrum, IEEE. (1998).

[38] MSDS: LITHIUM-ION BATTERIES. National Power Corporation, (2004)

[39] Henry, J.; Heinke, G. Environmental Science and Engineering; Prentice Hall, (1996).

[40] Newman, J.S.; Thomas-Alyea, K.E. Electrochemical Systems, Wiley-IEEE, 3rd ed. 2004

[41] Shiflett, M.B.; Yokozeki, A. Ind. Eng. Chem. Res. 44 (2005) 4453–4464.

[42] Kim, Y.S.; Choi, W.Y.; Jang, J.H.; Yoo, K.-.P.; Lee, C.S. Fluid Phase Equilib. 228–229 (2005) 439–445.

[43] Constantini, M.; Toussaint,V.A.; Shariati, A.; Peters, C.J.; Kikic, I. Journal of Chemical Engineering Data, 50 (2005) 52–55.

[44] Zhang, S.; Yuan, X.; Chen, Y.; Zhang, X. Journal of Chemical Engineering Data, 50 (2005) 1582–1585

[45] Zhang, J.; Zhang, Q.; Qiao, B.; Deng, Y. Journal of Chemical Engineering Data, 52 (2007) 2277–2283.

[46] Chen, Y.; Tarascon, J.M.; Guéry, C. Electrochemistry Communications, 2011. 13: P. 673-676.

[47] D. Pavlov, A. Kirchev, M. Stoycheva, B. Monahov, Journal of Power Sources 137

[48] Rogers, R.K.; Seddon, K.R. Ionic Liquids: Industrial Applications to Green Chemistry, Oxford University Press, Washington, DC, 2002.

[49] Rogers, R.K.; Seddon, K.R. Ionic Liquids as Green Solvents: Progress and Prospects, Oxford University Press, Washington, DC, 2003.

[50] Nyten, A.; Abouimrane, A.; Armand, M.; Gustafsson, T; Thomas. Journal of Electrochemical Communications, 2005, 7, 156–160.

[51] Yamada, A.; Iwane, N.; Harada, Y.; Nishimura, S.; Koyama, Y.; Tanaka, I. Advanced Material., 2010, 22, 3583.

[52] Gong, Z.; Yang, Y. Energy & Environmental Science, 2011, 4, 3223.

[53] Koltypin, M.; Aurbach, D.; Nazar, L.; Ellis, B. Journal of Power Sources, 2007, 174, 1241–1250.

[54] Dominko, R.; Bele, M.; Gaberscek, M.; Remskar, M.; Hanzel, D.; Goupil, J.M.; Pejovnik, S.; Jamnik, J. Journal of. Power Sources, 2006, 153, 274–280.

[55] Gong, Z.; Yang, Y. Energy and Environmental Science, 2011, 4, 3223

[56] Chen, J.J.; Whittingham, M.S. Electrochemical Communication, 2006, 8, 855–858.

[57] Recham, N.; Dupont, L.; Courty, M.; Djellab, K.; Larcher, D.; Armand, M.; Tarascon, J. M. Chemistry of Materials. 2009, 21, 1096–1107.

[58] Recham, N.; Chotard, J-N.; Dupont, L; Delacourt, C.; Walker, W.; Armand, M.; Tarascon, J.M. Nature Materials. 2010, 9, 68-74.

[59] Chen, Z.; Dahn,J.R. Journal of the Electrochemical Society, 149~9. (2002)

[60] Huang, H.; Yin, S.C.; Nazar, L.F. Electrochemical and Solid-State Letters, 2001;4:A170–2.

[61] Bewlay, S.I.; Konstantinov, K., Wang, G.X.; Dou, S.X.; Liu, H.K. Journal of Material Letter, 2004;58:1788–91.

[62] Roberts, M.R.; Spong, A.D.; Vitins, G.; Owen, J.R. Journal of Electrochemical Society, 2007;154:A921–8.

[63] Inagaki, M. Carbon 5 0 (2 0 1 2) 3 2 4 7 –3 2 6 6

[64] Huang H.; Yin, S.C.; Nazar, L.F. Electrochemical Solid State Letter, 2001;4:A170–2.

[65] Ravet, N.; Chouinard, Y.; Magnam, J.F.; Besner, S.; Gauthier, M.; Armand M. Journal of Power Sources, 2001;97:503–7.

[66] Franger,S.; Le Cras, F.; Bourbon, C.; Rouault, H. Electrochemical Solid State Letter, 2002;5:A231–2.

[67] Salah, A.; Mauger, A.; Zaghih, K.; Goodenough, J.B.; Ravet, N.; Gauthier, M. Journal of Electrochemical Society, 2003;153:A1692–701.

[68] Barker. J.; Saidi, M.Y.; Swoyer, J.L. Electrochemical Solid State Letter, 2003;6:A53–5.

[69] Doeff, M.M.; Hu, Y.; McLarnon, F.; Kostecki, R. Electrochemical Solid State Letter, 2003;6:A207–9.

[70] Bewlay, S.I.; Konstantinov, K.; Wang, G.X.; Dou, S.X.; Liu, H.K. Journal of Material Letter, 2004;58:1788–91.

[71] Yang, J.; Xu, J.J. Electrochemical Solid State Letter, 2004;7:A515–8.

[72] Myung,S.T.; Komaba, S.; Hirosaki, N.; Yashiro, H.; Kumagai, N. Electrochim Acta 2004;49:4213–22.

[73] Dominko, R.; Bele, M.; Gaberscek, M.; Remskar, M.; Hanzel, D.; Pejovnik, S. Journal of Electrochemical Society, 2005;152:A607–10.

[74] Striebel, K.; Shim, J.; Srinivasan, V.; Newman, J. Journal of Electrochemical Society, 2005;152:A664–70.

[75] Zhang, S.S.; Allen, J.L.; Xu, K.; Jow, T.R. Journal of Power Sources, 2005;147:234–40.

[76] Yang ,J.; Xu, J.J. Journal of Electrochemical Society, 2006;153:A716–23.

[77] Doeff, M.M.; Wilcox, J.D.; Kostecki, R.; Lau, G. Journal of Power Sources, 2006;163:180–4.

[78] Gabrisch, H.; Wilcox, J.D.; Doeff, M.M. Electrochemical Solid State Letters, 2006;9:A360–3.

[79] Shin, H.C.; Cho, W.I.; Jang, H. Electrochim Acta, 2006;52:1472–6.

[80] Roberts, M.R.; Spong, A.D.; Vitins, G.; Owen, J.R. Journal of Electrochemical Society, 2007;154:A921–8.

[81] Kim, K.; Jeong, J.H.; Kim, I.J.; Kim, H.S. Journal of Power Sources, 2007;167:524–8.

[82] Ong, C-W.; Lin, Y-K.; Chen, J-S. Journal of Electrochemical Society, 2007;154:A527–33.

[83] Kim, J.K.; Cheruvally, G.; Ahn, J.H.; Hwang, G.C.; Choi, J.B. Journal of Physical Chemistry Solids, 2008;69:2371–7.

[84] Kim, J.K.; Cheruvally, G.; Ahn, J.H.; Ahn, H.J. Journal of Physical Chemistry Solids, 2008;69:1257–60.

[85] Lin, Y.; Gao, M.X.; Zhu, D.; Liu, Y.F.; Pan, H.G. Journal of Power Sources, 2008;184:444–8.

[86] Liang, G.; Wang, L.; Ou, X.; Zhao, X.; Xu, S. Journal of Power Sources, 2008;184:538–43.

[87] Chen, Z.Y.; Zhu, H.L.; Ji, S.; Fakir, R.; Linkov, V. Solid State Ionics, 2008;179:1810–5.

[88] Wang, K.; Cai, R.; Yuan, T.; Yu, X.; Ran, R.; Shao, Z. Electrochim Acta, 2009;54:2861–8.

[89] Murugan, A.V.; Muraliganth, T.; Manthiram, A. Journal of Electrochemical Society, 2009;156:A79–83.

[90] Jaiswal, A.; Horne, C.R.; Cheng, O.; Zhang, W.; Kong, W.; Wang, L. Journal of Electrochemical Society, 2009;156:A1041–6.

[91] Nien, Y.H.; Carey, J.R.; Chen, J.S. Journal of Power Sources, 2009;193:822–7.

[92] Cho, Y.D.; Fey, G.T.K.; Kao, H.M. Journal of Power Sources, 2009;189:256–63.

[93] Palomares, V.; Goni, A.; de Muro, I.G.; de Meatza, I.; Bengoechea, M.; Cantero, I. Journal of Power Sources, 2010;195:7661–8.

[94] Kadoma, Y.; Kim, J.M.; Abiko, K.; Ohtsuki, K.; Ui, K.; Kumagai, N. Electrochim Acta, 2010;55:1034–41.

[95] Zhou, X.; Wang, F.; Zhu, Y.; Liu, Z. Journal of Materials Chemistry, 2011;21:3353–8.

[96] Fey, G.T.K.; Huang, K.P.; Kao, H.M.; Li, W.H. Journal of Power Sources, 2011;196:2810–8.

[97] Peng, W.; Jiao, L.; Gao, H.; Qi, Z.; Wang, Q.; Du, H. Journal of Power Sources, 2011;196:2841–7.

[98] Jugovic, D.; Mitric, M.; Kuzmanovic, M.; Cvjeticanin, N.; Skapin, S.; Cekic, B. Journal of Power Sources, 2011;196:4613–8.

[99] Rui, X.H.; Jin, Y.; Feng, X.Y.; Zhang, L.C.; Chen, C.H. Journal of Power Sources, 2011;196:2109–14.

[100] Toprakci, O.; Ji, L.; Lin, Z.; Toprakci, H.A.K.; Zhang, X. Journal of Power Sources, 2011;196:7692–9.

[101] Fromhold, A.T. Jr.; Cook, E.L. Physical Review, 158, 600–612 (1967)

[102] Yao, H. J.; Elder, K. R.; Guo, H; Grant, M. Physical Review B, 1993; 47-21.

[103] Masquelier, C; Wurm, C; Rodriguez-Carvajal, J; Gaubicher, J; Nazar, L. Chemical Materials 2000, volume 12, pages 525-532

[104] Streltsov, V. A; Belokoneva, E. L; Tsirelson, V. G; Hansen, N. K. Acta Crystallographica Section B. pages 147-153 (1993)

7.0 Glossary

$1s^2 2s^2 2p^6 3^1$: Electron orbitals

$1s^2 2s^2 2p^6 3^5$: Electron orbitals

AA, AAA, C, and D batteries: Commercial sizes of batteries used in certain electronic devices.

AAO: Anodized Aluminum Oxide template used to facilitate growth of nanowires during electrochemistry

AgCl: silver chloride

$AgNO_3$: silver nitrate

Amps: a measurement of current where 1 A is 1culomb/second.

C: carbon

C (1,2,3… etc): Rate for charging and discharging. A 1C rate would charge the battery in one hour and discharge the battery in one hour. A 3C rating would charge the battery in 20 minutes.

Cl: chlorine ion

Cl_2: chlorine gas

CVD: chemical vapor deposition

DFT: density functional theory

DI: de-ionized

EDS or EDX: Energy Dispersive X-ray Spectroscopy

Fe: Iron

FeCl: Iron(II) Chloride$^-$

$FeCl_3$: Iron(III) Chloride

$FePO_4$: Iron Phosphate

G: gram

GaP: gallium phosphate

H: Hydrogen ion

$H_2NH_2PO_4$: dihydrogen ammonium phosphate

H_2SO_4: sulfuric acid

HPLC: High pressure liquid chromatography

KeV: kilo electron volt

KOH: potassium hydroxide

Li: lithuim

Li/C: lithium carbon composite

LiCl: lithium chloride

Li_xCoO_2: Lithium Cobalt Oxide the first commercially available cathode material used in lithium ion batteries. Not all Lithium atoms can intercalate into the crystal structure, which results in a ratio described as “x” in Li_xCoO_2.

$LiFePO_4$: Lithium Iron Phosphate is an insulating olivine naturally found in the mineral Triphylite

$LiFePO_4$/C: Lithium Iron Phosphate Carbon composite used as a cathode material in lithium ion batteries

$Li_3Fe_2(PO_4)_3$: unstoicheometric lithium iron phosphate

$LiNi_{0.5}Mn_{1.5}O_2$: lithium nickel manganese oxide

LiOH: lithium hydroxide

$LiPF_6$: lithium phosphor hexofloride

Li_3PO_4: lithium phosphate

M: molarity

mA: Milliamp is the amount of current or charge available per unit time available to do work. Commercially, the time parameter is in hours. 1 ampere= 1000 milliamps

mA*h: Milliamp hour is used to describe the total amount of current that can be held within a battery system.

mA*h/g Specific Capacity: The total amount of current a material can hold per unit mass

mL: milliliters

mg: milligram

mol: Avagadro's number (6.022 X 10^23) of molecules

mol/L: moles per liter (also known as molar concentration)

mtorr: A definition of pressure where 760 torr equals 1 earth atmosphere of pressure.

NaCl Sodium chloride: an ionic salt commonly referred to as table salt comprised of sodium and chlorine atoms. When dissociated sodium receives a positive charge and chlorine receives a negative charge (Na^+ Cl^-)

nm: nanometer

μm: micrometer

O: oxygen

P: Phosphorous

$PbSO_4$: lead sulfate

RPM: revolutions per minute

SEM: Scanning Electron Microscope used to take optical images in the micron to nanometer scale

SiO_2: silicon dioxide

sp^2 hybridized: Referring to the electronic orbital of an atom, in our case carbon, bonded to three other atoms.

Volts: Electromotive force that explains the driving force between 2 terminals.

W/Kg: Specific Energy, used to describe the rate of charging/discharging per unit mass.

Wh/kg: Specific Power, used to describe how much energy a storage device can hold per unit mass.

Watts: Measurement of Power

Wh/kg: Specific power per kilogram

XRD: X-ray Diffraction